DEVELOPMENT OF COPPER AND MANGANESE DOPED TERNARY COLLOIDAL QUANTUM DOT ALLOYS

A Thesis Submitted to
the Graduate School of Engineering and Sciences of
İzmir Institute of Technology
in Partial Fulfillment of the Requirements for the Degree of

MASTER OF SCIENCE

in Chemistry

by
İlayda Melek YIRTICI

January 2019
İZMİR

We approve the thesis of **İlayda Melek YIRTICI**

Examining Committee Members:

Prof. Dr. Serdar ÖZÇELİK
Department of Chemistry, İzmir Institute of Technology

Assoc. Prof. Dr. Ali ÇAĞIR
Department of Chemistry, İzmir Institute of Technology

Assoc. Prof. Dr. İlbeyi AVCI
Department of Physics, İzmir Ege University

29 January 2019

Prof. Dr. Serdar ÖZÇELİK
Supervisor,
Department of Chemistry
İzmir Institute of Technology

Prof. Dr. Ahmet Emin EROĞLU
Head of the Department of Chemistry

Prof. Dr. Aysun SOFUOĞLU
Dean of the Graduate School of
Engineering and Sciences

ACKNOWLEDGMENTS

First of all, I would like to thank my supervisor Prof. Dr. Serdar ÖZÇELİK and for their guidance, suggestions, patience, encouragement and support throughout my thesis study.

I would like to thank Dr. Seçil Sevim ÜNLÜTÜRK with all my heart for endless help, guidance and always smiling face. Besides, I would like to thanks to my lab mates Dr. Özge TUNCEL ÇERİK, Almila YÜKSEL and Hande UÇAK for their helps and their friendships.

My special thanks to all friends at IZTECH especially Büşra YILDIZ, Seray Ece KESKİN, Özlem ECE, Elif GÜREL and Yunus Emre AYDIN for endless encouragement and never ending friendship.

Finally there are no words to express my deep and endless thank to my family, my mother Serpil ElGÜN YIRTICI, my father Kadri YIRTICI. I would like to thank my grandfather Muharrem ELGÜN a million times, even though he couldn't see my graduation while he was still alive.

ABSTRACT

DEVELOPMENT OF COPPER AND MANGANESE DOPED TERNARY COLLOIDAL QUANTUM DOT ALLOYS

Semiconductor nanocrystals have great interest due to their unique optical properties such as the particle size and the alloy composition dependent spectra, photochemical and colloidal stability. They have wide range of potential applications like solar cells, light emitting diodes (LED) and bioimaging etc. In this thesis, colloidal ternary Cu doped and undoped ZnS_xSe_{1-x} nanoalloys were synthesized by modified one pot aqueous approach. TGA and MPA ligands were used as capping agents for the synthesis of ZnS_xSe_{1-x} and Cu doped ZnS_xSe_{1-x} colloidal nanoalloys. The results showed that capping agents have an significant effect on optical properties of ZnS_xSe_{1-x} nanoalloys. Although the TGA capped nanoalloys have well-defined absorption bands rather than MPA capped ones, ZnS_xSe_{1-x} nanoalloys with TGA capping agent fluorescence peak was not observed. Therefore, the further study was continued with MPA capped ZnS_xSe_{1-x} ternary nanoalloys. Optical spectra demonstrated both absorption and PL spectra were shifted due to the adding of Cu dopant. Absorption peak shifted from 335 nm to 376 nm. Fluoroscence spectra also was redshift from 469 nm to 565 nm. Thus, we can conclude that, colloidal ternary nanoalloys optical properties can be tuned by using chemical doping. On the other hand, the optical and structural properties of binary ZnSe QDs, Mn and Cu doped ZnSe nanocrystals were investigated. We concluded that ZnSe and ZnS_xSe_{1-x} nanocrystals can be used to synthesize doped nanocrystals by chemical doping. We demonstrated that optical and structural properties of Cu and Mn doped ZnSe can be tuned by chemical doping.

ÖZET

BAKIR VE MANGAN KATKILI ÜÇLÜ KOLLOİDAL KUANTUM NOKTA ALAŞIMLARININ GELİŞTİRİLMESİ

Yarı iletken nanokristaller, parçacık boyutu ve alaşım bileşimine bağlı spektrum, fotokimyasal ve kolloidal stabilite gibi benzersiz optik özelliklerinden dolayı büyük ilgi görmektedir. Güneş pilleri, ışık yayan diyotlar (LED), biyo görüntüleme vs. gibi çok çeşitli potansiyel uygulamalara sahiptirler. Bu tezde, üçlü kolloidal nano alaşımlar bakır katkılı ve katkısız olarak, tek adımda ve su ortamında sentezlenmiştir. ZnS_xSe_{1-x} ve Cu katkılı ZnS_xSe_{1-x} kolloidal nano alaşımlar, TGA ve MPA organik ligandları kullanılarak sentezlenmiştir. Sonuçlar göstermektedir ki, farklı organik ligandların kullanılması, sentezlenen ZnS_xSe_{1-x} üçlü alaşımların optik özelliklerini etkilemektedir. TGA organic ligandı kullanılarak sentezlenen nano alaşımın soğurma bandı daha belirgin olsa da, emisyon piki gözlenmemiştir. Bu yüzden devam eden çalışmalarda MPA organic ligandı kullanılarak sentezlenen ZnS_xSe_{1-x} üçlü nano alaşımı kullanılmıştır. Cu katkısının eklenmesine bağlı olarak, soğurma ve ışıma spektrumlarında kayma gözlenmiştir. Soğurma piki 335 nanometreden 376 nanometreye kayarken , emisyon piki de 469 nanometreden 565 nanometreye kayma göstermiştir. Sonuç olarak, üçlü kolloidal nano alaşımların optik özelliklerinin kimyasal katkılandırma ile değiştirebileceğini söyleyebiliriz. Öte yandan, ikili ZnSe QD, Mn ve Cu katkılı ZnSe nanokristallerinin optik ve yapısal özellikleri incelenmiştir. ZnSe ve ZnS_xSe_{1-x} nanokristallerinin, katkılı nanokristalleri kimyasal dopingle sentezlemek için kullanılabileceği sonucuna vardık. Cu ve Mn katkılı ZnSe'nin optik ve yapısal özelliklerinin kimyasal dopingle ayarlanabileceğini gösterdik.

TABLE OF CONTENTS

LIST OF FIGURES

LIST OF TABLES

CHAPTER 1
INTRODUCTION

1.1. Nanotechnology and Nanocrystals

Nanotechnology, as a recent field of science, can be described as controlling and observing the behavior of molecules and atoms ranging between 0.1 nm and 100 nm. The origin of nanotechnology has its roots back 1960, when Richard Feynman, an American physicist, lectured "There's Plenty of Room at the Bottom''. He claimed that scalable materials could be replicated to molecular scale. [1]

Even though nanoscience and nanotechnology, as a term, has become to known more recently, chemists has actually been studying over 20 years. The most common examples of this technology are polymers, and the computer chips that are used on daily basis. Nowadays, nanotechnology is particularly being studied in the fields of electronics, medicine and solar cells. The broad application range of nanotechnology is based on the fact that this technology actually allows controlling of individual atoms and molecules.[2]

Nanocrystals or nanoparticles with size of smaller than a micron (1-100nm) display unique optical, electronic and chemical properties owing to their small sizes and high/volume surface ratio. Colloidal semiconductor nanocrystal, a special type of nanocrystals named as quantum dots (QDs), shows these properties between bulk semiconductors and discrete atom or molecules which is called confinement effect. These quantum dots can be synthesized in different compositions, shapes, sizes and internal structures, resulting in various properties. For example, QDs can be obtained at specific wavelength by simply adjusting the size of the nanoparticles. More specifically, whereas QDs with 2-3 nm size emit shorter wavelengths which blocks the color between blue and green, QDs with relatively larger size about 5-6 nm emit longer wavelength, allowing the color to shift orange and red Figure 1.1 [3-4].

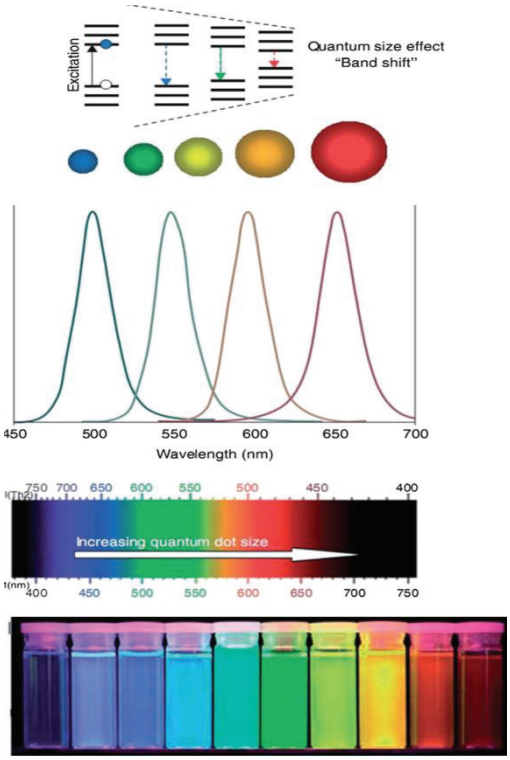

Figure 1.1 Size-dependent PL colors of semiconductor QDs. [4]

Nanocrystals are usually consist of elements from groups III–V, II–VI, or IV–VI of the periodic table, such as CdS, CdSe, CdTe, CdS/ZnS, CdSe/ZnS, CdSeTe/ZnS. Quantum dots could be classified as doped quantum dots, core and core / shell type quantum dots. Core type semiconductor nanocrystals includes at least two atoms such as CdTe, CdSe, CdS, ZnTe, ZnS, etc. Since 1980 various methods have been developed to synthesize Quantum dot. However, different synthesis methods have been tried due to the electronic defects on the surface and poor crystallinity. [4]

In 1993, Murray et al. produced high quality nearly monodisperse particles like CdS,CdSe,CdTe based on pyrolysis of organometallic reagents by injection. Higher emission wavelengths can be observed due to surface traps on quantum dots. Such surface traps diminish the quantum yield and also cause to broad fluorescence range.[5]

To reduce the negative effects of surface traps and enhance the quantum yield, core/shell or doped semiconductors can be used. In core /shell semiconductors, quantum dot core is covered by other semiconductor which has wider band gap to increase the photostability and luminescence properties.[6]

In the beginning, CdSe/ZnS and CdSe/CdS are the mostly studied. In addition, these CdSe/ZnSe, CdTe/CdS CdTe/ZnS, and even CdTe/CdS/ZnS can be developed

as“core/shell/shell” QDs. The first synthesized core shell was CdSe / ZnS by using organometallic reagents and the quantum yield has been increased up to 50% [7]

Another way to tune the electronic and optical properties of quantum dots are doping of nanocrystal with transition metal ions. Doped quantum dots cannot be affected to thermal, chemical, and photochemical disturbances [6]. Mn and Cu, as a transition metal dopants, are mostly used for doping of semiconductors. According to litrerature, composition-tunable near-infrared emitting Cu-doped CdS quantum dots was synthesized by one-pot aqueous synthesis method. In this study $CdCl_2$ and $CuCl_2$ were mixed together and the ph was adjusted to 8.0 by using NaOH. Then Na_2S solution was added as a S precursor. After Cu doping, the emission peaks shifted from 649 nm to 722nm. [8]

Due to their band gap dependent properties, quantum dots are capable of being applied in many areas like optoelectronics, photovoltaics, and biological imaging. However, for some specific applications, very small nanocrystals are necessary. Therefore, it is difficult to tune the properties of quantum dots without regarding size. Alter of semiconductor band gap can be made by changing composition of nanocrystals. This situation can be overcome by using alloy semiconductor nanocrystals without changing quantum dot size[9-10] .

Zhong et al. (2003) synthesized $Zn_XCd_{1-X}Se$ alloyed semiconductor nanocrystals which was showed high luminescence and stability properties. Their synthesis based on starting with CdSe nanocrystals, then adding Zn and Se ions at high temperature. With the increase of the Zn content, blue shifts were observed in the emission wavelength. As a result, they obtained alloy nanocrystals possessing good PL properties in the blue spectral range and also keeping their high luminescence in the aqueous solution. [11]

Sharma et.al (2013) synthesized CdSe/ZnSe core-shell and $Zn_xCd_{1-x}Se$ ternary alloy nanocrystals by using one pot and double pot synthesis procedure. They used one pot synthesis approach to formation of both CdSe/ZnSe core shell and $Zn_xCd_{1-x}Se$ ternary alloy nanocrystals. Depending on the percentage of zinc added, the properties of the nanocrystals have changed. Red shift was occurred due to the changing of the Zn content from 0 to 10 at % for core shell nanocrystals. In addition, quantum yield increased respect to CdSe core. After the Zn content increased above 20%, blue shift was observed due to the formation of the ternary alloy structure $Zn_xCd_{1-x}Se$ at the emission wavelength.

However, for double pot synthesis, increasing Zn content from 10 to 40 at % caused red shift for the core-shell nanocrystals. Besides, blue shift was not observed because ternary alloy structure was not formed. As a result, CdSe-ZnSe core shell

nanocrystals which has same concentration of Zn content synthesizing by one pot procedure display high PL intensity, narrow FWHM. [12]

1.2. Basics of Colloidal Synthesis

Colloidal semiconductor nanocrystals are synthesized by many different methods recently. Most of the synthesis based on the chemical reactions between cation and anion precursors.[3] Different synthesis methods provide to obtain quantum dots with different optical properties.

There are mainly four chemical synthesis methods which are organometallic approach, two phase approach, solvothermal approach and one pot aqueous approach. In this thesis, one pot method and two phase method were applied.

1.2.1. Two Phase Approach

Nowadays, thanks to usage of low-toxicity and low-cost reagents, two phase method is mostly preferred to organometallic approach and also this method is more environmental-friendly and economical[13] .The most important advantage of this method is that the synthesis can be done at low temperature and is controllable. The CdS nanocrystal which was first nanocrystalline synthesized by the two-phase method. [14]

Pan et al. (2007) synthesized also CdS, CdSe and CdSe/CdS core-shell nanocrystals which was oil-soluble by using different precursors such as NaHSe, Na_2SeSO_3, and Na2S. Nanocrystals was arised in the toluene- water interface. [15] The schematic representation of reaction mechanism for CdSe nanocrystals were shown in Figure 1.2 .

1.2.2. One Pot Aqueous Approach

Aqueous synthesis is cheaper, less toxic and water-soluble rather than orgonometallic synthesis. These synthesis procedure was developed by Gaponik et al. They synthesized thiol-capped CdTe NCs in water.[16] Another study in the literature, blue-ZnSe nanocrystals synthesized was studied by Huang et al. (2013). They used Na_2SeO_3 instead of NaHSe as a Se source. GSH was used both as stabilizing agent and reducing agent.[17] Schematic presentation of the synthesis of blue emitting ZnSe nanocrystals were shown in Figure 1.3.

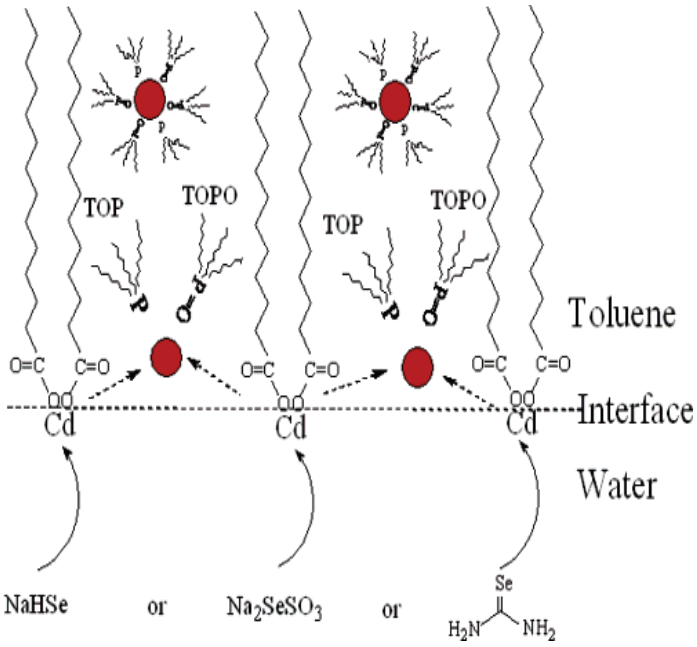

Figure 1.2 The chemical mechanism of CdSe nanocrystals by using different precursors at water-toluene interface.[15]

Zhang et al. also studied core shell ZnSe/ZnS quantum dots in aqueous solution. They prepared TGA capped ZnSe QDs with cationic inverse injection method. In order to obtain core/shell ZnSe/ZnS QDs, they used epitaxial overgrowth method in an aqueous solution. They investigated effect of pH value, the molar ratio of ZnSe/thiourea and refluxing time to obtain high quality core–shell ZnSe/ZnS QDs.

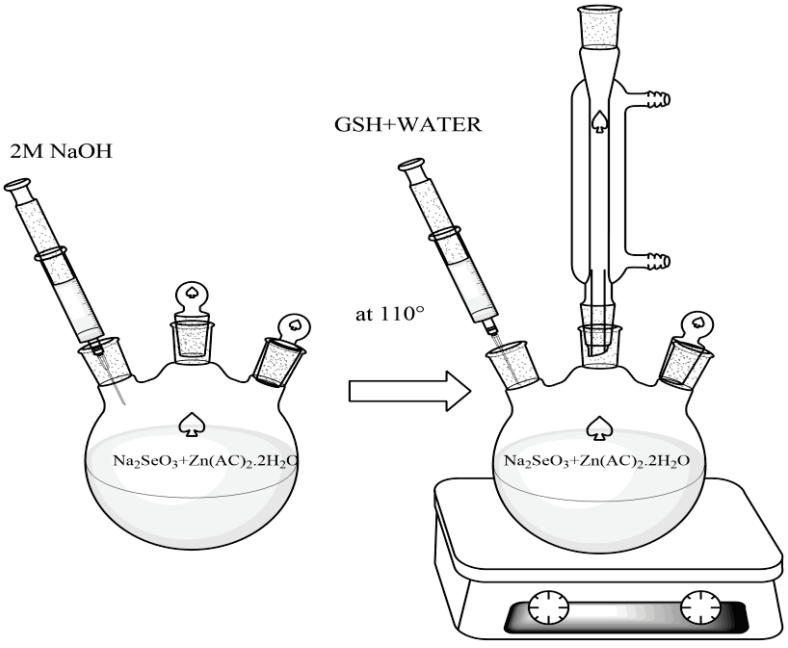

Figure 1.3 Schematic presentation of the synthesis of blue emitting ZnSe nanocrystals.

1.3. Characterization of Nanocrystals

1.3.1. Optical Characterization

Absorption of visible and ultraviolet (UV) radiation is associated with excitation of electrons, in both atoms and molecules, from lower to higher energy levels. Different molecules absorb energy at different wavelengths. For each wavelength the intensity of light passing through both a reference cell and the sample cell is measured. Absorbance is basically a logarithmic ratio of initial radiation to transmitted radiation through the material. According to Beer Lambert Law absorbance is proportional to the concentration, the extinction coefficient of the material and length of the light path.

Fluorescence is brought about by absorption of photons in the singlet ground state promoted to a singlet excited state. The excited states are short lived with a lifetime at about 10^{-8} seconds because of unchanged of electron spin in fluorescence. Fluorescence occurs at wavelengths longer than that of the excitation radiation.

Figure 1.4 shows one form of Jablonski diagram. In this figure, S_0, S_1 and are singlet excited states. The lighter horizontal lines represent of vibrational levels. As shown in Figure 1.4, absorption transitions can occur from the ground singlet electronic state (S_0) to various vibrational levels of the excited singlet electronic states (S_1 and S_2). After the light absorption several processes usually occur such as internal conversion, fluorescence, intersystem crossing etc. The excited electron return to the lowest vibrational level of ground state (S_0) which is called fluorescence.

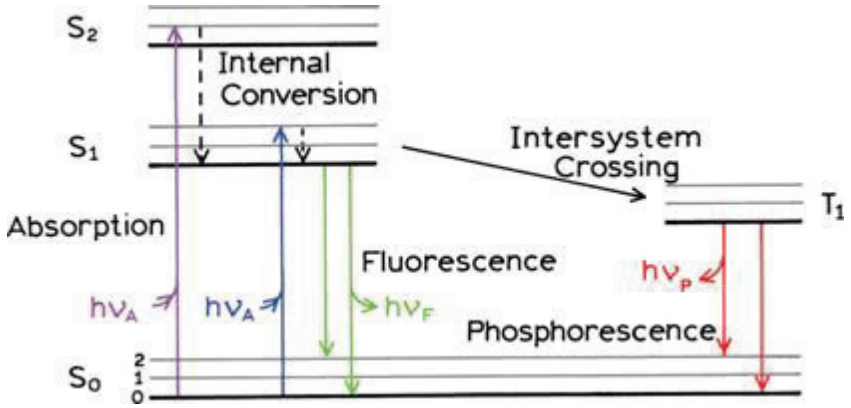

Figure 1.4 One form of Jablonski diagram.

An emission spectrum is the wavelength distribution of an emission measured at a single constant excitation wavelength. This spectra can be presented as either a wavelength scale or a wavenumber scale. The wavelength can be easily converted to the wavenumber or vice versa.

The equation below shows the quantum yield calculation formula which is simply the ratio of the number of emitted photons to the number of absorbed photons.[18]

$$QY = \frac{Number\ of\ emitted\ photons}{Number\ of\ absorbed\ photons} \tag{1.1}$$

Quantum yield and lifetime measurements could be understood by Jablonski diagram as shown in Figure 1.5. In this diagram indicate that emission of sample could be occurs by radiative and non-radiative process.

The following equation can be used to calculate the quantum yield. At this figure, k_r and k_{nr} and are the rate constants of radiative and non-radiative processes of the sample, respectively. [18]

$$QY = \frac{k_r}{k_{nr}+k_r} \tag{1.2}$$

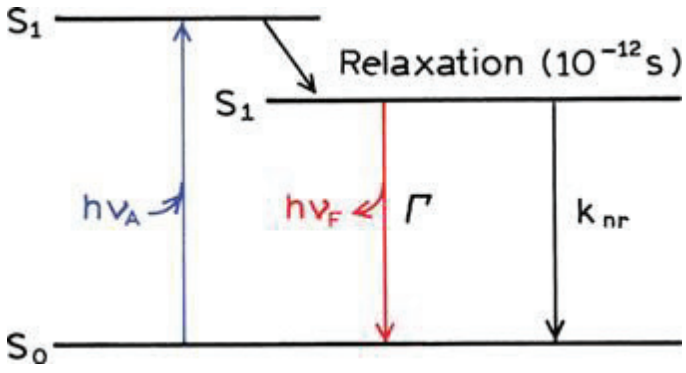

Figure 1.5 An example of Jablonski diagram to understand of quantum yields and lifetimes.

The standard dye with well-known quantum yield is used to calculate the quantum yield. However, we used an integrated sphere to measure quantum yield in our experiments.

Another important parameter for optical characterization is time resolved measurements. In many cases like the overlap of emission and absorption spectra, time-resolved measurements provide more information than steady-state measurements. The measurements are performed by TCSPC which is time correlated single photon counting. Basically, the excitation of sample by a pulse of light and then the measurement of time between excitation of sample and observation of photons.

1.3.2. Structural Characterization

There are many methods used for the structural characterization of quantum dots such as X-Ray Diffraction (XRD), Transmission Electron Microscopy (TEM) etc.

Structural characterization of synthesized semiconductor quantum dots was carried out by using X-Ray Diffraction (XRD), Dynamic Light Scattering (DLS) technique, Scanning Electron Microscopy-Energy Dispersive X-Ray Spectroscopy (SEM-EDS).

X-Ray Diffraction (XRD) measurements were carried out by Philips X-pert Pro Powder Diffractometer at IYTE-MAM (Material Research Center). XRD is one of the non destructive technique to reveal information about the chemical composition and crystal structure of the nanocrystals. XRD is X-ray based technique where the material interacts with X ray beam of specific wavelength. The beam gets scattered depending on the crystal structure of the sample and generates a plot having intensity as a function of 2 theta. Nanocrystals were purified with isopropanol and centrifugation technique, then powdered form of the nanocrystals were used for XRD analysis.

Scanning Electron Microscopy was used to obtain compositional information about the nanocrystals. In EDS the X rays are generated due to interaction between electron beam and the sample. Their intensities as a function of energy are monitored. Each element has a specific "fingerprint" energy level. In order to do this, Energy Dispersive X-Ray Detector (EDS), the most common accessory of SEM was used. FEI Quanta 250 FEG Scanning Electron Microscope at IYTE-MAM is used for the analysis.

The size of the nanocrystals were investigated by Dynamic Light Scattering (DLS) Measurements by Malvern Zetasizer Nanoseries -Nano-ZS. Actually, DLS instrument gives the information about size distribution of small particles in solution. Generally, the results obtained from DLS was bigger than the results obtained from TEM

or STEM. The reason of that, TEM measures the hard core of the nanocrystal but DLS measures both the hard core and the hydrodynamic diameter of the nanocrystals.[19]

1.4. Purpose of This Study

The purpose of the study is to change the optical properties of nanocrystals by chemical doping. Copper and Manganese doped ZnSe/ZnS nanocrystals were investigated. In addition Copper doped ZnS_xSe_{1-x} ternary quantum dot alloys were synthesized to understand differences between binary quantum dots and ternary alloys by chemical doping.

CHAPTER 2
SYNTHESIS AND CHARACTERIZATION OF CU DOPED ZnSSe ALLOY NANOCRYSTALS BY TWO PHASE APPROACH

2.1. Introduction

Colloidal semiconductor nanocrystals have attracted many years researchers' attention due to their optical and magnetic properties. They have great potential applications in biological detection, light emitting diodes and sensors etc.[20] Since QDs of CdTe, CdSe, HgSe, HgCdTe have been widely studied by many groups. However, the toxicity of these materials limits their applications in biological and particularly medical environments. Therefore, the researchers have shown a tendency towards the zinc based quantum dots.

ZnSe and ZnS are the most studied II–VI semiconductor nancrystals. ZnS nanocrystals have high PL emission in UV-blue region. [21] Thanks to the wide band gap and large binding energy of ZnSe, they are used widely for passivation shell for another type of quantum dots to improve the stability and PL emission.[21-22] Alloy has three or four elements which can be classified as either ternary (3 elements) or quaternary (4 elements). Ternary alloys have two binary systems with either common anion or cation. For instance, considering the $Zn_xCd_{1-x}Se$ alloy structure, M′A and M″A produces $M'_xM''_{1-x}A$, where M′ and M″ are two different cations and A is the common anion. Alloying of MA′ and MA″,where M is the common cation while A′ and A″ are two different anions is produced $MA'_xA''_{1-x}$ nanoalloys like CdS_xSe_{1-x}.

Alloyed semiconductors display properties both of the their bulk counterparts and also their parent semiconductors part. As a result, alloyed nanocrystals have additional properties that are dependent on the composition, except for the properties resulting from quantum confinement effects.[10] ZnS_xSe_{1-x} nanoalloys have a great potential to control the energy bandgap and the lattice constants of ZnSe and ZnS binary QDs in one system. Doping of ternary semiconductor nanoalloys by using foreing atoms provides enhancement in the functionalities of QDs.

2.2. Methods

ZnS_xSe_{1-x} colloidal nanoalloys were synthesized by using one pot aqueous method. Then, synthesized nanocrystals doped with copper by partial cation exchange reaction.

2.2.1. Reagents

Copper(II) chloride and zinc chloride were purchased from Sigma Aldrich as a metal sources. Se powder (Sigma) and sodium borohydride ($NaBH_4$, Sigma) were used for forming NaHSe solution. Thiourea (Sigma), 3-mercaptopropionic acid (MPA,Sigma), thioglycolic acid were used. 2-proponol for purification of nanoalloys was also purchased from Sigma Aldrich.

2.2.2. Synthesis of $ZnS_x Se_{1-X}$ Ternary Nanoalloys

In order to synthesis ZnS_xSe_{1-x} nanocrystals, first of all, Se precursors was prepared. In this process, Se powder and sodium borohydride were used.

2.2.2.1. Synthesis of Se Precursor, NaHSe

The reaction between sodium borohydride and selenium were shown in the below. Sodium borohydride oxidized by selenium.

$$4\ NaBH_{4(s)} + 2\ Se_{(s)} + 7\ H2O_{(l)} \longrightarrow 2\ NaHSe_{(aq)} + Na_2B_4O_{7(s)} + 14\ H_{2(g)} \qquad (2.1)$$

Due to the high sensitivity of NaHSe to the air, the reaction must take place under nitrogen or argon gas at room temperature. In this synthesis, 1.2 mmol Se powder and 2.5 mmol $NaBH_4$ were mixed with 10 ml ultra-pure water in and nitrogen gas atmosphere. After approximately an hour clear solution of 2.5 mL NaHSe was used in order to synthesize of colloidal nanoalloys.

2.2.3. Synthesis of Colloidal ZnS_xSe_{1-x} Ternary Nanoalloys

The ternary nanoalloys were synthesized by using one pot aqueous method [16] with small modifications. For this experiment, two flasks were prepared. 3 mmol $ZnCl_2$ was dissolved in 110 ml pure water. Thioglycolic acid (TGA) and mercaptopropionic acid (MPA) used as capping agent for each of them. 6 mmol mercaptopropionic acid was added to each of the flask. pH of the solution was adjusted to 10 by dropwise additon of 1 M of NaOH solution. pH value is crucial for this reaction because if the pH was not adjusted to 10, cloudy solution was observed for MPA capped ZnS_xSe_{1-x} ternary nanoalloys. The flask was attached to the condenser in order to provide reflux with under N_2 atmosphere for an hour at 80°C. After one hour reflux time, thiourea and freshly synthesized NaHSe were injected at the same time into the reaction flask as S and Se precursors, respectively, and the reaction temperature was increased to 110°C. Sample of aliquots taken at different time intervals were monitored by UV–Vis spectra for their optical properties. The reaction was stopped by cooling the reaction flask.

2.2.4. Synthesis of Colloidal Cu-Doped ZnS_XSe_{1-x} Ternary Nanoalloys

0.02 M $CuCl_2$ solution in ultra pure water was prepared as Cu precursor. Zn: Cu mole ratio was adjusted to 2. Then, Cu^{+2} solution was added into the ZnS_xSe_{1-x} reaction flask at 110 ˚C under N_2 atmosphere after 20 hours. Schematic representation of the synthesis was shown Figure 2.1. While the growth of particles continue, aliquots of samples were taken at different time interval. After obtaining the desired particle size and the absorption wavelengths, purification procedure was applied.

2.2.5. Purification of Doped and Undoped ZnS_XSe_{1-x} Ternary Alloys

In order to eliminate excess reactants and impurities purification must be implemented. After both of the reaction was stopped, isopropanol was added to the reaction in 1:1 volume ratio. Centrifugation at 6000 rpm for 15 minutes was applied to obtain precipitated QDs.

After centrifugation, supernatants were removed and resulted precipitate were dried at room temperature.

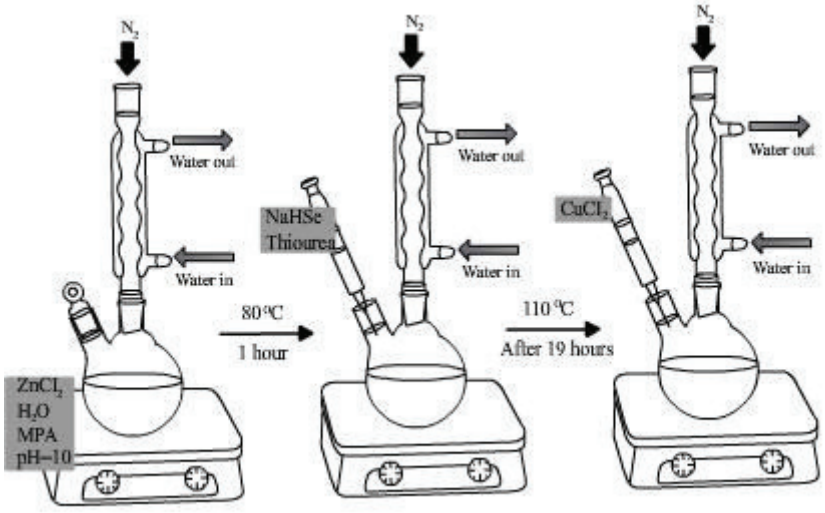

Figure 2.1 Schematic representation of synthesis Cu doped ZnSxSe1-x ternary nanoalloy.

2.3. RESULTS & DISCUSSION

2.3.1. Optical Characterization

Absorption and photoluminescence spectra of the ZnS_xSe_{1-x} and Cu^{2+} doped ZnS_xSe_{1-x} nanoalloys were obtained by FS5 Edinburgh Spectrofluorometer. This analysis was performed to control reaction proceeding.

Figure 2.2 display the absorption spectra of water dispersible MPA capped ZnSSe ternary nanoalloys. It can be seen that absorption band shows red shift from 342 nm to 385 nm.

In Figure 2.3 TGA capped colloidal ZnSxSe1-x nanoalloys show that absorption edge shifted 316 nm to 326 nm which indicates the growth of nanoparticles. The differences in absorption peak of TGA capped ZnSSe and MPA capped ZnSSe are showed effects of capping agent.

When MPA was used as capping agent the colloidal nanoalloys displayed PL emission after 170 minutes of reaction time with an excitonic emission peak at 360 nm and the peak centered around 410 nm as the trap emission. Besides both of the peaks shifted with the reaction time.

When TGA was used as capping agent there was no emission peak observed. These results indicate that, capping agents play significant role in the PL properties of colloidal ZnSxSe1-x nanoalloys.

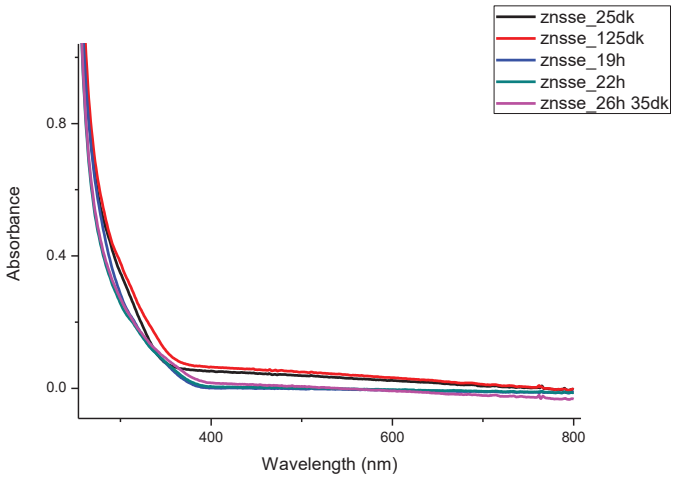

Figure 2.2 The absorption spectra of MPA capped $ZnS_{0.74}Se_{0.26}$ nanoparticles at different time interval.

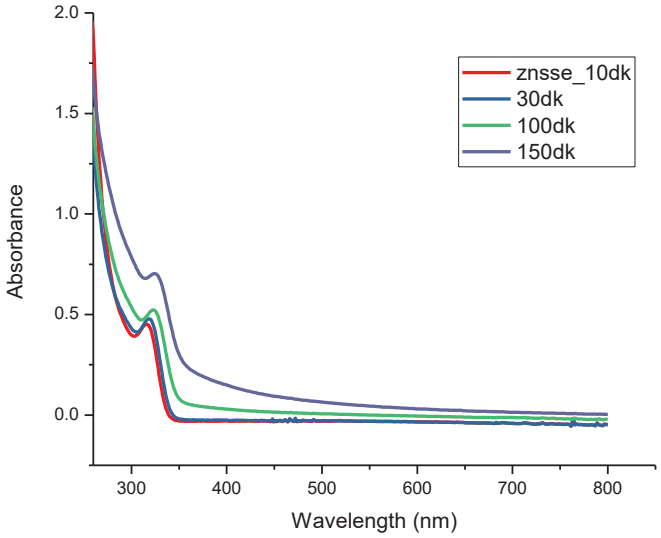

Figure 2.3 The absorption spectra of TGA capped $ZnS_{0.48}Se_{0.52}$ nanoparticles with respect to the reaction time.

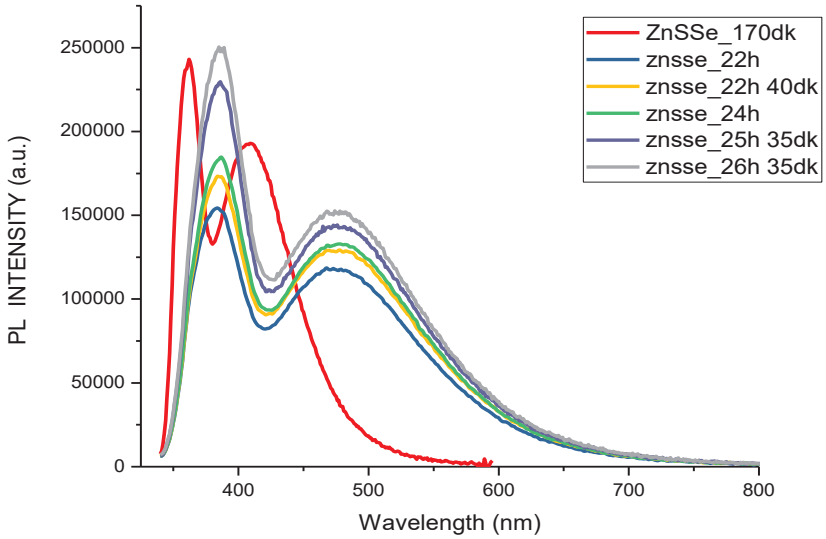

Figure 2.4 PL spectra of MPA capped $ZnS_{0.74}Se_{0.26}$ nanoalloys with respect to the reaction time.

It can be seen from the Figure 2.5, absorption band shifted from 346 nm to 380 nm after addition of 2 % Cu dopant. However, there is no significant differences in absorption peak position with the reaction time. For MPA capped nanoalloys, first excition band in the absorption spectrum is nearly unclear. Some reports claim that this propertyless absorption spectra should originate from the absorption of the host nanocrystal.[23] However, it can be seen that, when changed the capping agent, band shapes of the absorption spectra was changed.

Figure 2.6, show the normalized PL intensity of Cu doped $ZnS_{0.94}Se_{0.06}$ nanoalloys. Like in absorption spectra, fluorescence emission spectra also showed the red shift as shown in Figure 2.6. The PL intensity of the excitonic emission at 388 nm of $ZnS_{0.94}Se_{0.06}$ NCs was quenched with doping of Cu impurity. The reason of this situation, photoinduced excitons are more easily trapped by Cu impurities[24] .

The trap state emission was exhibited at the 450 nm after the addition of Cu dopant. During the approximately 200 minute of the reaction, no red shift was observed. However, after the 300 minute of the reaction the trap state emission showed clearly red shift from 469 nm to 565 nm with the reaction time. The photograph show that at the end of the reaction, Cu doped ZnSSe nanoalloys were exhibited green luminescence property.

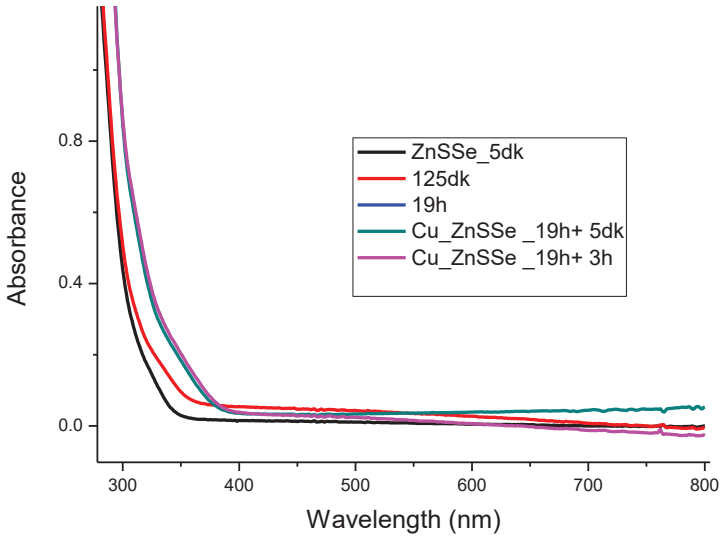

Figure 2.5 Absorption spectra of %2 Cu doped $ZnS_{0.94}Se_{0.06}$. Absorption spectra was shifted from 346 nm to 380 nm.

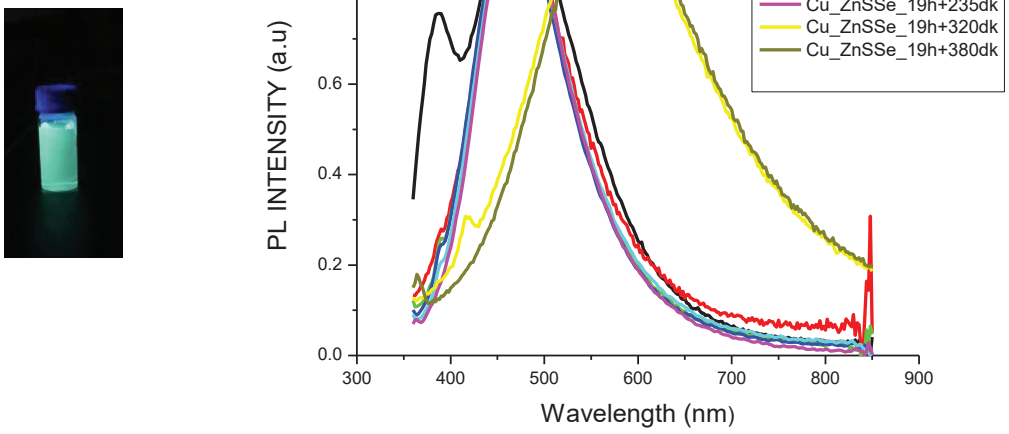

Figure 2.6 Normalized Fluorescence spectra of $ZnS_{0.94}Se_{0.06}$:Cu nanoalloy . Zn:Cu initial mol ratio 3:0.02. Photographs of Cu doped ZnS_xSe_{1-x} nanoalloys under UV illumination.

Photoluminescence Quantum Yield of Cu doped ZnS_xSe_{1-x} nanocrystals were measured by using integrated sphere. Figure 2.7 show the photoluminescence quantum yield of ZnS_xSe_{1-x} nanocrystals. PL QY % of ZnS_xSe_{1-x} nanocrystals increased up to 2.5 % after 19 hour of reaction. Than decreased to 1 % during the reaction. This is also expectable that when the reaction time increases, size of nanocrystals also increase and some defect states started to form which causes the decrease in quantum yield of nanocrystals. As shown in figure 2.7, The PL QY % of Cu doped ZnS_xSe_{1-x} nanoalloys higher than ZnS_xSe_{1-x} nanocrystals. The Cu doped ZnS_xSe_{1-x} nanoalloys reached the maximum quantum yield value after the addition of copper dopants into the reaction. However, the PL QY % of Cu doped ZnS_xSe_{1-x} began to decreasing during the reaction. At the end of the reaction, the quantum yield of Cu doped ZnS_xSe_{1-x} was 2.79%.

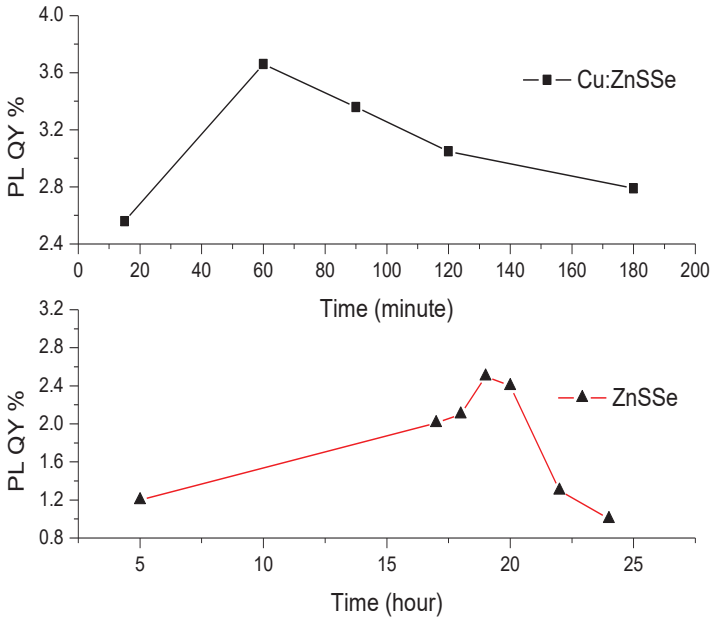

Figure 2.7 Comparison of photoluminescence quantum yield of Cu:ZnSSe nanoalloys and ZnSSe NCs. Initial mole ratio of Zn:Cu was 3:0.02.

Table 2.1 show the the lifetime results with each components at the wavelength of 450 nm, 457 nm, 500 nm, 520 nm respectively. Three or four exponential fitting procedure was applied to reach the best $\chi 2$ value as close to 1. Average lifetime values

were calculated by relative percents of each components and shown in Table 2.1. According to the results, fast and slow processes have approximately same lifetime values.

Figure 2.8 showed that the lifetime values versus wavelength of the Cu doped ZnSSe nanoalloys. This graph indicated that Cu doped ZnSSe nanoalloys reached the maximum lifetime values at the wavelength of 457 nm which was 52 ns.

Table 2.1 Fluorescence lifetime values for Cu doped ZnSe nanocrystals.

Sample	Initial Cu:Zn mole ratio	τ_1 ns	Rel %	τ_2 ns	Rel %	τ_3 ns	Rel %	τ_4 ns	Rel %	$\tau_{average}$ ns
Cu:ZnSSe	0.02:3	0,1970	1433,365	3,84	128,1	43,57	82,02	59,09	-59,8	35
Cu:ZnSSe	0.02:3	0.198	1597,943	5,25	79,48	55,91	29,55	-	-	52
Cu:ZnSSe	0.02:3	0.207	1728.918	19.8	66.13	-	-	-	-	48
Cu:ZnSSe	0.02:3	0.2043	1434,24	4,13	125,1	49,79	7,56	-	-	38

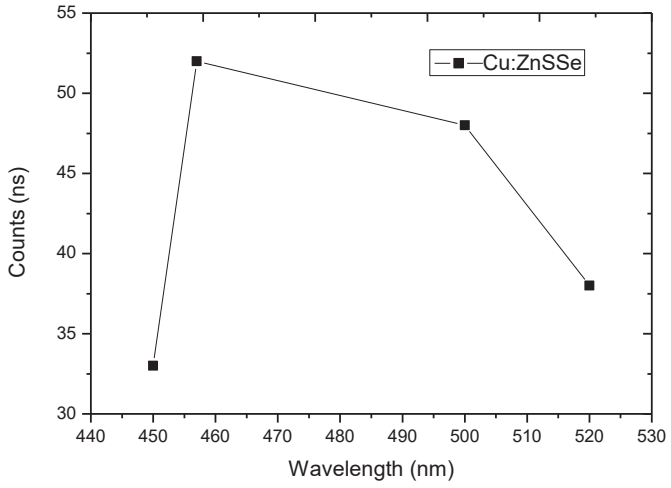

Figure 2.8 Lifetime values versus wavelength of Cu doped ZnSSe nanocrystals. The best lifetime values were obtained at the wavelength of 457 nm.

2.3.2. Structural Characterization

Structural characterization of Gd doped CdTe nanocrystals was done by Dynamic Light Scattering (DLS) instrument, X-Ray diffraction (XRD) analysis and Scanning Electron Microscopy – Energy Dispersive X-Ray Spectroscopy (SEM-EDS).

Cu doped ZnS_xSe_{1-x} nanoalloys was purified with isopropanol and centrifugation as mention in Section 2.2.5. SEM-EDS analysis were carried out for these purified nanocrystals in order to obtain compositional information.

SEM-EDS analysis confirmed that Cu^{2+} ions were doped into ZnS_xSe_{1-x} nanoalloys. By SEM-EDS measurements, the amount of Cu^{2+} ions with respect to Zn ion incorporated into the QDs as an atomic percent was calculated as 1.7 % when the initial Cu^{2+} mole percentages were of 2 %.

Table 2.2 SEM-EDS result of Cu doped ZnSSe nanoalloys.

Sample	Inıtial Zn:Cu mole ratio	SEM-EDS Results
Cu:ZnSSe	3:0.02	$Cu_{1.7}Zn_{98.3}S_{0.73}Se_{0.27}$

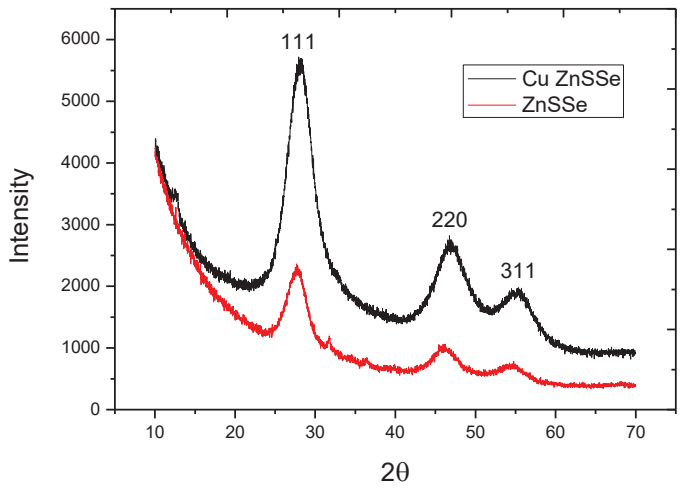

Figure 2.9 XRD patterns of synthesized ZnSSe NCs and %2 Cu doped ZnSSe nanoalloys which are cubic and have zinc blende structure.

XRD spectroscopy is carried to understand the structure and the composition of the nanocrystals. Figure 2.9 show that both ZnSSe and Cu doped ZnSSe nanocrystals are cubic and have zinc blende structure. These diffraction features appearing at 28,0, 46.7,

and 55.1 corresponded to the (111), (220), and (311) planes of cubic zinc blende structure. This results prove that the lattice of the ZnSSe host material is intact after doping with Cu^{+2} ions.

The size of the nanoparticles were measured by DLS technique. In order to measure size of the Cu doped ZnSSe nanoalloys, the samples were centrifuged firstly. Then, samples were redispersed in water. Before the measurement, samples were sonicated and it was passed through microfilter. Figure 2.10 show that ZnSSe and 2% Cu doped ZnSSe nanoalloys were measured as 17 nm and 32 nm respectively.

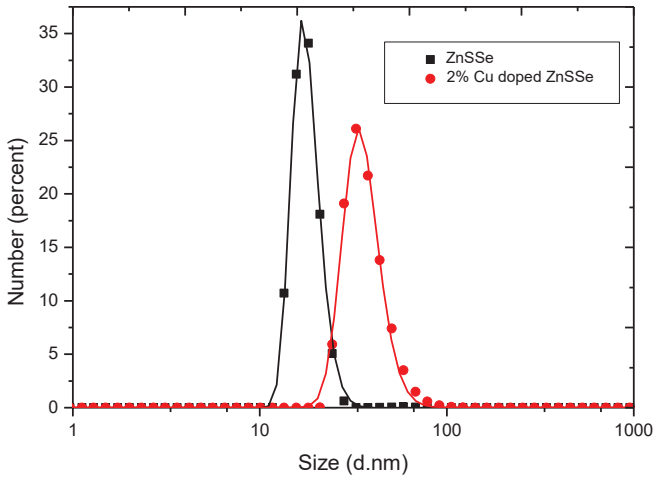

Figure 2.10 DLS result of ZnSSe and Cu doped ZnSSe nanocrystals. The nanocrystal size was increased after addition of copper dopant.

2.4. Conclusion

One pot aqueous synthesis method was used to synthesize MPA capped Cu doped ZnS_xSe_{1-x} nanoalloys. Initial Cu:Zn mole ratio was 0.02:3. Absorption and photoluminescence spectra was obtained for optical characterization. The quantum yield of ZnS_xSe_{1-x} and Cu doped ZnS_xSe_{1-x} were obtained by using integrated sphere. PL QY % of Cu doped ZnSSe higher than ZnSSe NCs. The lifetime value showed that, Cu doped ZnSSe nanoalloys reached the maximum point at the wavelength of 457 nm. Size of Cu doped ZnSSe nanoalloys also obtained from DLS technique which showed that addition of copper ion resulted increase in the size of nanocrystals up to 32 nm. SEM-EDS result proved the Cu content in nanocrystals.

CHAPTER 3
SYNTHESIS AND CHARACTERIZATION OF Cu AND Mn DOPED ZnSe NANOCRYSTALS

3.1. Introduction

II–VI semiconductor nanocrystals known as quantum dots demostrate excellent electronic and optoelectronic properties. The cadmium based QDs such ad CdSe, CdTe etc, has been investigated so far. However, this QDs were found toxic and dangerous for the human body and the environment in time. Therefore, lower toxic zinc compounds have attracted much interest by researchers.[22]

Tuning of the properties of QDS can be achieved by varying the size of the semiconductor, changing composition or by incorporating transition metal impurity into the host lattice. Doped ZnSe QDs can be synthesized by both orgonometallic route and aqueous phase route. However, using aqueous based approach has been considered as a mild and green route chemistry comparing with organometallic route.[25]

Transition metal ions like Cu and Mn have been used as dopant to nanocrystals in order to enhance the optical properties of quantum dots like minimazing self-absorption, having narrower PL emission spectra or provide better thermal stability. There are several reports in the literature about doped semiconductor. Xue et al[20],synthesized Cu doped ZnSe quantum dots by growth doping mechanism in aqueous solution. Transition metal ions doped core / shell nanocrystals also studied in literature. Cu doped ZnSe/ZnS core shell nanocrystals were synthesized by Shuhong et al.[26] In this study, ZnSe core synthesized with using MPA as a capping agent firsty. Then ZnS shell was deposited around the synthesized quantum dots under N2. The produced nanocrystals demonstrated excellent stability and higher quantum yield than Cu doped ZnSe nanocrystals. Quantum yield was up to from 5 % to 8.9 %. Another study was reported by Luong et al.[27] They synthesized ZnSe/ ZnS:Mn core/(doped) shell nanocrystals succesfully. They controlled optical and electronic properties of nanocrystals based on by regulating feeding molar ratio [Zn]/[Mn]. At the end of this experiment, they obtained three different emission colors like green, orange and white colors thanks to the alteration of initial molar ratio [Zn]/[Mn].

3.2. Experimental

ZnSe colloidal QD's were synthesized by using one pot aqueous method. Then, synthesized nanocrystals doped with copper and manganese ions.

3.2.1. Reagents

Copper(II) chloride, manganese (II) chloride tetrahydrate and zinc chloride were purchased from Sigma Aldrich as a metal sources. Se powder (Sigma) and sodium borohydride ($NaBH_4$, Sigma) were used for forming NaHSe solution. Thiourea (Sigma), Sodium sulfide, 3-mercaptopropionic acid (MPA,Sigma), Thioglycolic acid were used for synthesis. 2-proponol for purification of nanoalloys was also purchased from Sigma Aldrich.

3.2.2. Synthesis of Mn doped ZnSe Nanocrystals

Water soluble Mn doped ZnSe nanocrystals synthesized with the similar method, one pot aqueous approach that was discussed in section 2.2.3. For this experiment, three flasks were prepared. Firstly, ZnSe core was synthesized by using $ZnCl_2$, MPA and NaHSe solution in water. Briefly, 1 mmol $ZnCl_2$ was dissolved in 110 ml pure water. Mercaptopropionic acid (MPA) used as capping agent. 2 mmol MPA was added to each of the flask. pH of the solution was adjusted to 10 by dropwise additon of 1 M of NaOH solution. Then, the flasks were attached to the condenser in order to provide reflux with under N_2 atmosphere for an hour at 80°C. Se precursor was injected into the reaction flask after an hour and the reaction temperature was increased to 110°C.

For doping procedure, aqueous Mn^{2+} stock solutions were prepared at different concentrations using $MnCl_2 .4H_2O$. Different amount of Mn^{2+} solutions (Mn^{2+} at % relative to Zn^{2+} 2 %, 15 % and 40 % respectively.) were injected into the ZnSe reaction flask at 110 ˚C under N_2 atmosphere following the ZnSe core formation (approximately 20 hours later). Aliquots of sample were taken at different time interval.

3.2.3. Synthesis of Cu doped ZnSe Nanocrystals

Water dispersible Copper doped ZnSe nanocrystals were synthesized by two different procedure. In method a, ZnSe core was synthesized the same way that was

discussed in section 3.2.2. For doping procedure, Copper (II) chloride used to prepared stock solutions. As-prepared stock solutions as 2% and 5% added to reaction flask separately after 20 hours approximately. The reaction flask was heated at 110˚C under the nitrogen atmosphere. Aliquots of the sample were taken at different time intervals and their optical properties were monitored by UV–Vis spectra.

In method b, copper doped ZnSe quantum dots have synthesized with using different synthesis procedure. Briefly, $ZnCl_2$, MPA and $CuCl_2$ were mixed and the pH of the solution was adjusted to 10 by using 1M NaOH solution. The flasks were attached to the condenser in order to provide reflux with under N_2 atmosphere for an hour at 80°C. Then, NaHSe solution was injected into the reaction flask and the reaction temperature was increased to 110°C.

3.2.4. Capping ZnS Shell on Mn Doped ZnSe Nanocrystals

After that, due to the air sensitivities of ZnSe nanocrystals, ZnS shell was added on the Mn Doped ZnSe nanocrystals. For coating procedure, 0.05 mmol $ZnCl_2$ and 0.05 mmol sodium sulfide were prepared separately in ultrapure water. Then adding slowly to the reaction flask under stirring. The reaction was terminated by cooling after 4 hours of the injection of ZnS shell precursors. The reaction was stopped by cooling the reaction flask to the room temperature.

3.2.5. Purification of Mn Doped ZnSe Nanocrystals

Precipitation process was the same Cu doped ZnS_xSe_{1-x} ternary nanoalloys which discussed in section 2.2.5. After the reaction was stopped/quenched, isopropanol was added to the reaction in 1:1 volume ratio to precipitate the QDs. Precipitated QDs were obtained by centrifugation and the supernatant was removed. The precipitated QDs were dried in room temperature in order to get powdery QDs. The dried powder may be stocked either as prepared or redispersed in aqueous dispersions with desired concentration.

3.3. RESULTS &DISCUSSION

Result and Discussion part were divided into two parts which is optical characterization and structural characterization of Mn doped ZnSe NCs and Cu doped ZnSe nanocrystals.

3.3.1. Optical Characterization

Optical characterization of Mn doped ZnSe nanocrystals were performed by lifetime measurements, UV-Vis Absorption and fluorescence spectroscopies. Aliquots were taken in different time intervals to control the reaction.

Taken optical spectra for Mn doped ZnSe nanocrystals with initial Zn:Mn mole ratio as 1:0.02 is shown in Figure 3.1. Absorbance spectra showed that, the addition of manganese ions did not cause a very effective change in the absorbance band. Due to ZnSe stabilized by MPA capping agent synthesized in aqueous phase, ZnSe QDs exhibit emission band in the region of 440–500 nm assigned to the surface trap emission.[27] However, after the addition of 2% manganese ion, the trap emission shifted slightly from 493 nm to 500 nm and also PL intensity of trap state was increased because of addition of extra hole to the core ZnSe quantum dots.

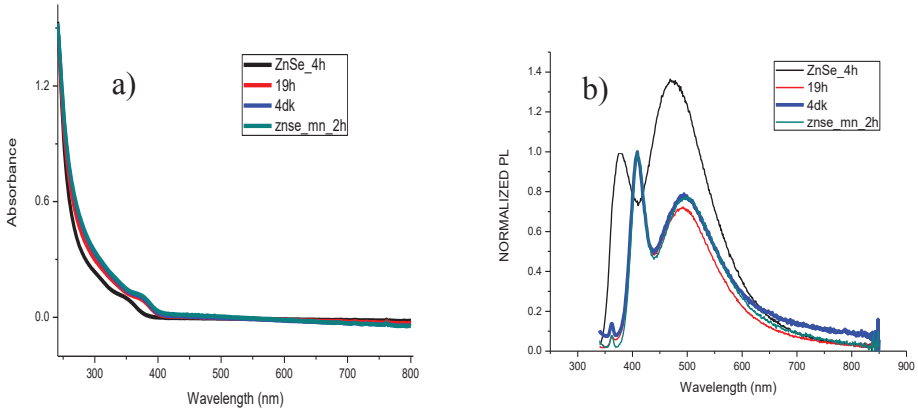

Figure 3.1 (a) Absorption and (b) Normalized PL spectra of Mn doped ZnSe nanoalloys with respect to reaction time. Zn:Mn mole ratio was 1:0.02 respectively.

2% Mn doped ZnSe QDs show green luminescence property because of trap state emission. However, surface trap state emission of these QDs can be controlled with dopant concentration. Luong et al, states that increasing dopant concentration provides pseudo-tetrahedral ($^4T_1$ to $^6A_1$) transition of Mn^{2+} ions which causes to QDs show yellow-orange color. [27]

Figure 3.2 and Figure 3.3 show absorption and photoluminescence spectra of MPA capped ZnSe with doping of manganese ion (15%), respectively. As in 2%

manganese additives there is no significant change in absorbance peaks. For PL spectrum, both of the excitonic and trap states shifted slightly. After four hours, PL intensity has decreased dramatically because of quenching manganese ion, however.

Zinc sulphide (ZnS) shows extraordinary photoelectric and luminescent properties due to owing to a large band-gap energy (3.66 eV). To determine the effect ZnS shell coating on the ZnSe core, the shell layer was grown on the core structure. The growth of a ZnS shell around ZnSe QDs could improve its optical properties. ZnS shell did not induce any spectral feature on the absorption spectra however, PL intensity was increased significantly.

Luong state that [27], different size of Mn^{+2} and Zn^{+2} ions effect the surface defects of ZnSe quantum dots at low Mn dopant concentrations. Figure 3.4 shows absorbance spectra of %40 Mn doped ZnSe/ZnS nanocrystals. Absorbance spectra display similar trend in %2 Mn doped ZnSe and %15 Mn doped ZnSe nanocrystals. Absorbance spectra shifted from 355 nm to 361 nm after incorporation of manganese ions.

Figure 3.5 indicates that photoluminescence emission spectra of ZnSe QDs with the emission peak at 389 nm. Band gap emission at 360-400 nm and surface trap emission at 450-500 nm. Addition of manganese ions were provided shifted emission spectra 400 nm. However, PL intensity was decreased sharply due to quench effect of high concentration of manganese ion. In order to improve that, ZnS shell adding on to Mn doped ZnSe nanocrystals. After one hour addition of ZnS shell was lead to enhancemet of PL intensity. In addition, trap state emission shifted from 500 nm to 491 nm after adding of ZnS shell (after 1 h). This blue shifting was indicate that ZnS shell was formed on to Mn doped ZnSe nanocrystal.

Table 3.1 Photoluminescence Quantum Yield of Mn doped ZnSe and ZnSe/ZnS.

Sample	Inıtıal Zn:Mn Mole Ratio	Quantum Yield Reaction Medium	Quantum Yield After Purification
Mn:Zn	1:0.02	15,4 %	1,4%
Mn:Zn	1:0.15	12,7%	1,8%
Mn:Zn	1:0.40	10,7%	1,56%

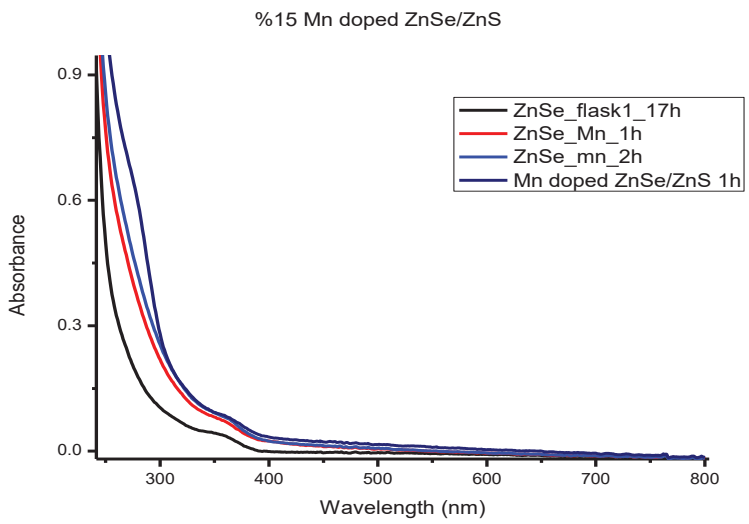

Figure 3.2 Absorption spectra of Mn doped ZnSe/ ZnS nanocrystals with respect to reaction time. Inıtial mole ratio of Zn:Mn was adjusted as 1:0.15.

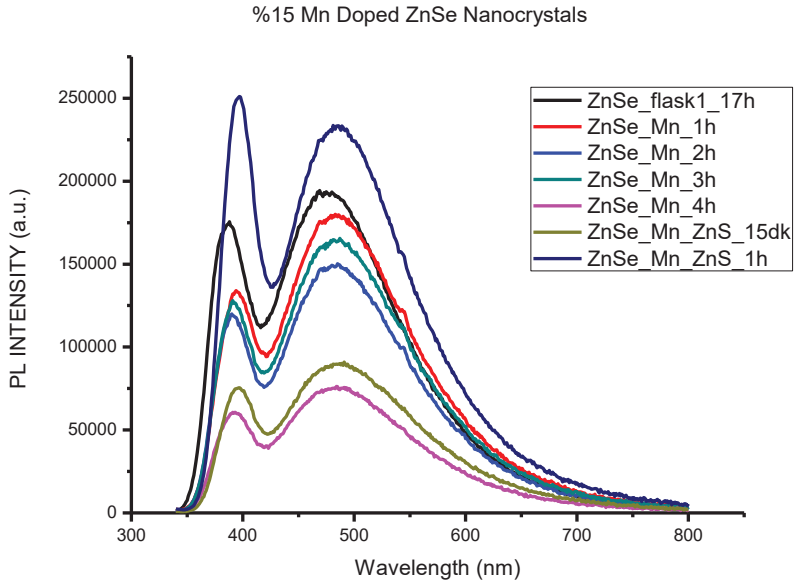

Figure 3.3 Photoluminescence spectra of Mn doped ZnSe/ZnS nanocrystals. PL intensity was increased after addition of ZnS shell.

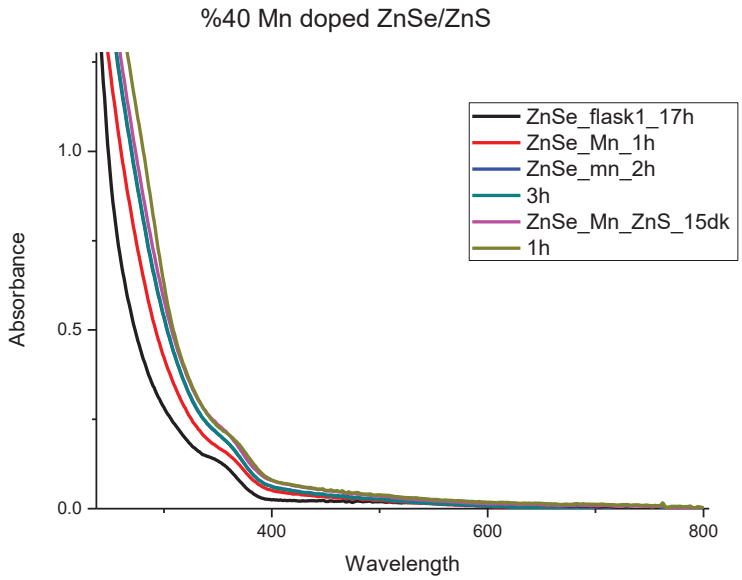

Figure 3.4 Absorption spectra of Mn doped ZnSe/ZnS nanocrystals. The molar ratios of Zn:Mn was 1:0.40.

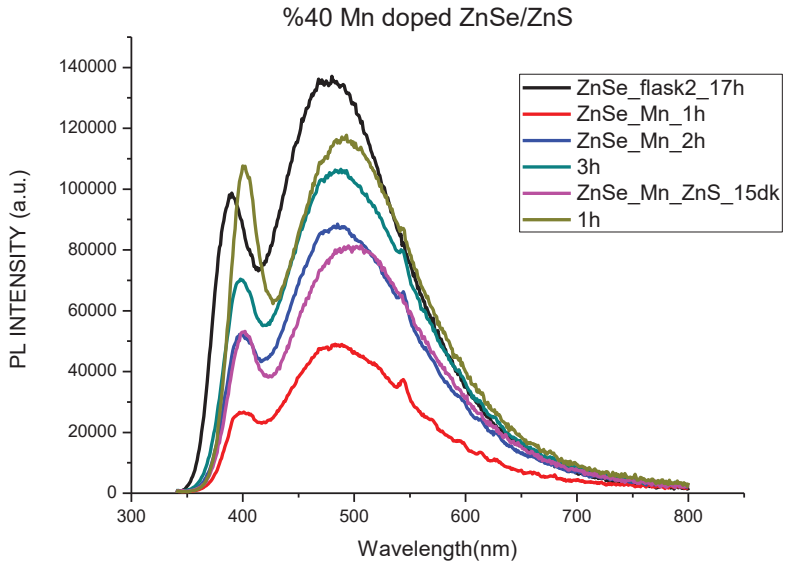

Figure 3.5 Photoluminescence spectra of Mn Doped ZnSe/ZnS nanocrystals. The ZnS shell was added three hours after the addition of manganese ion.

As it given in Table 3.1 photoluminescence quantum yield of nanocrystals showed a significant difference when Mn content added to ZnSe nanocrystals. ZnSe QDs can be synthesized both orgonometallic and aqueous method. As prepared ZnSe QDs with orgonometallic route shows high QY % and good monodispersity. However, this reaction method requires high reaction temperature, toxic reagents and solvents.[28] In contrast, ZnSe QDs synthesis with water based approach display water-dispersible properties and also this method can be conducted mild reaction temperature. (<150°C). However, the obtained water-soluble QDs usually have low quantum yield[29]. The water based route synthesis of ZnSe QDs show quantum yield of near zero or <1 after purification [30]. The reason of low quantum yield is many trap states on the surface of the QDs[31].

In addition, the stability of NCs is controlled by the probability of photoinduced holes being present on the nanocrystal surface. However, doping of Mn impurities into the ZnSe nanocrystal was lead to decreasing quantum yield. The reason of this, due to the presence of hole trappers of Mn impurities were caused increasing probability of holes being present on the NC surface.[24]

The another reason could be the environmental factors. Wang et al. states that, photoirridation and oxygen affecting the chemical stability of doped ZnSe nanocrystals. The interaction of photoirradiation and oxygen results in the precipitation of doped ZnSe nanocrystals. As a result, quantum yield of doped ZnSe NCs are very low due to the instability of nanocrystals.

In order to obtain photodynamic information fluorescence decay traces were taken for ZnSe/ZnS and Mn doped ZnSe/ZnS nanocrystals. Three exponential fitting procedure was applied to reach the best $\chi 2$ value as close to 1. The lifetime results with each component are shown in Table 3.2. According results, fast and slow processes have approximately the same lifetime values. Average lifetime values were calculated by relative percents of each components and shown in Table 3.2. Average lifetime values showed that, adding 15% Manganese ion gave the best result for lifetime measurement.

Taken both of the tables, the fluorescent decay traces were consistent with quantum yields of Mn doped ZnSe/ZnS nanocrystals.

Figure 3.6. showed absorbance spectra of Cu doped ZnSe/ZnS nanocrystal synthesized with by using method a. Zn^{+2}/Cu^{+2} mole ratio was adjusted 1: 0.02. After adding of Cu impurities to the flask, the wavelength shifted from 370 nm to 378 nm rapidly. Covering Cu doped ZnSe with the ZnS shell allowed the wavelength to shift from 373 nm to 382 nm.

Table 3.2 Fluorescence lifetime values for ZnSe/ZnS and Mn doped ZnSe/ZnS nanocrystals. $\chi 2$ values are between 1,314 and 1,599.

Sample	Zn/Mn Mole ratio	τ1 (ns)	Rel %	τ2 (ns)	Rel %	τ3 (ns	Rel %	τaverage (ns)
ZnSe/ZnS	-	0,2365	31,68	3,4709	61,17	15,1552	7,15	3,28
Mn:ZnSe	1: 0.02	0,2176	61,31	3,4456	33,28	27,3308	5,42	2,76
Mn:ZnSe/ZnS	1: 0.15	0,2034	79,52	3,9051	11,68	50000	8,80	5
Mn:ZnSe/ZnS	1: 0.40	0,2037	87,57	3,9566	6,00	42,9607	6,44	3,18

Evidence of successful copper doping in ZnSe QDs has been deduced from PL measurements. Figure 3.7 PL spectra of Cu doped ZnSe/ZnS nanocrystal. The trap states was disappeared immediately after addition of Cu dopants. show the emission spectra of Cu doped ZnSe/ZnS nanocrystals. For ZnSe NCs, an obvious bandgap emission around 400 nm and a defect emission around 480 nm can be observed. The emission peak formed at 536 nm was formed after the addition of the copper dopant. The reason of this situation, photoinduced excitons are more easily trapped by Cu impurities as confirmed by ref 31.

Gong et al [29] states that, , Changing of PL intensity with time and stability of dopant emission point out that the Cu^{2+} ions are internal-doped in the ZnSe NCs. They were suggested that, doping of NCs consist of two steps such as surface adsorption of dopant and the followed internal doping.Firstly, host ZnSe nanocrystals formed. after growing of host nanocrytals, dopant ions were introduced on the surface of host nanocrystals .Consequently, surface-doped nanocrystals is formed. As the reaction continured, ZnSe maintained of growth on the surface of doping layer and formed the internal doped ZnSe:Cu nanocrystals. Therefore, if the more Cu^{+2} ions are introduced into the ZnSe nanocrystals, the stronger fluorescence intensity was observed according to internal doping mechanism.

Figure 3.9 shows the light emitting mechanism of Cu doped ZnSe nanocrystal.According to this, electrons are occured between the valance band and $3d^9$ ground state of Cu^{+2} and conduction band of ZnSe nanocrystal. After ZnSe absorbs the energy, the electrons on the valence band jump to the conduction band. After that, electron comes to the level of energy generated by the impurity ions ($Cu^{2+)}$ and relaxes there. Finally, electron jump o the T^2 level of Cu^{2+} to illustrate green photoluminescence property.

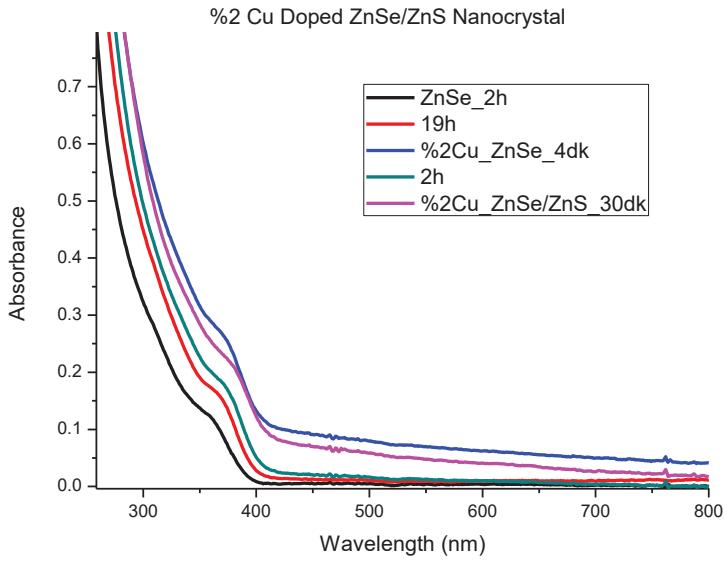

Figure 3.6 Absorption spectra of Cu doped ZnSe/ZnS nanocrystals. Initial mol ratio of Zn:Cu was 1:0.02. The applied synthesis procedure was method a.

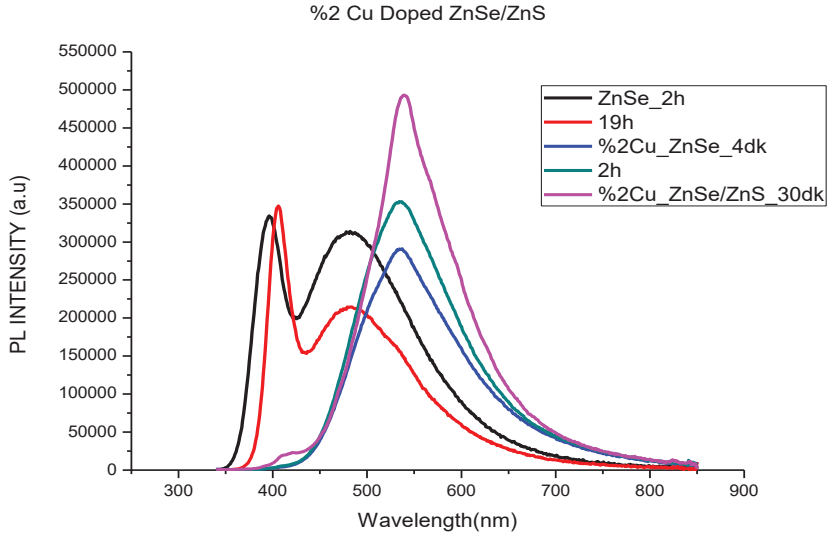

Figure 3.7 PL spectra of Cu doped ZnSe/ZnS nanocrystal. The trap states was disappeared immediately after addition of Cu dopants.

As shown from in Figure 3.8 Cu doped ZnSe/ZnS nanocrystals show green luminescence properties which is discussed above. Cu doped ZnSe QDs show two emission peaks. One of them was sharp emission peak at 400 nm was assigned to the band gap emission of ZnSe nanocrystal. The other broad peak at 480 nm was came from ZnSe QDs trap emission. However, after doping of Cu^{+2} ions, both of the emission peaks were disappeared, as shown in Figure 3.7. The strong emission peak at 536 nm was formed, and PL emission changed from blue to green obviously, which is the characteristic emission peak of Cu^{2+} ions.

Absorption spectrum of 5% Cu doped ZnSe nanocrystals was shown in Figure 3.10. Adding of Cu^{+2} ions were resulted in shifted wavelength from 346 nm to 359 nm. However, there was a nonzero baseline was occurred at 800 nm after 5% Cu doping. The reason of that, Cu:ZnSe core NCs rapidly precipitate from the solution over 3 hours. This situation leads to the scattering of large aggregates and absorption spectra was observed like Figure 3.10[26].

Figure 3.11 showed ZnSe QDs have similar emission peaks like 2% Cu doped ZnSe NCs. There was excitonic (or bandgap) emission at 380 nm and a defect emission at 473 nm observed. After doping of Cu impurities, there was only an emission peak at 443 nm. Although there was no change in the optical density value, PL intensity was decreased sharply, however. The reason of that could be if the reaction time is too long, more Cu atoms diffused on the surface of ZnSe nanocrystals. This leads to a reduction in the luminescence center and also cause to surface defects. As a result, the nanocrystalline luminescence intensity decreases [29].

a) Under Daylight **b) Under UV light**

Figure 3.8 a) from right to left image shows ZnSe QDs (at reaction time 2h and 19h) under day light. In figure b, from right to left image shows ZnSe (2h and 19h), Cu doped ZnSe (4dk-2h) and Cu:ZnSe/ZnS (30dk) under UV light.

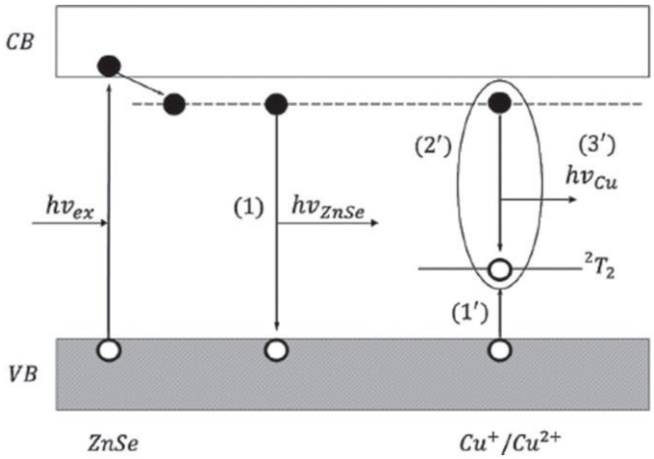

Figure 3.9 Light emitting mechanism of Cu doped ZnSe nanocrystals.

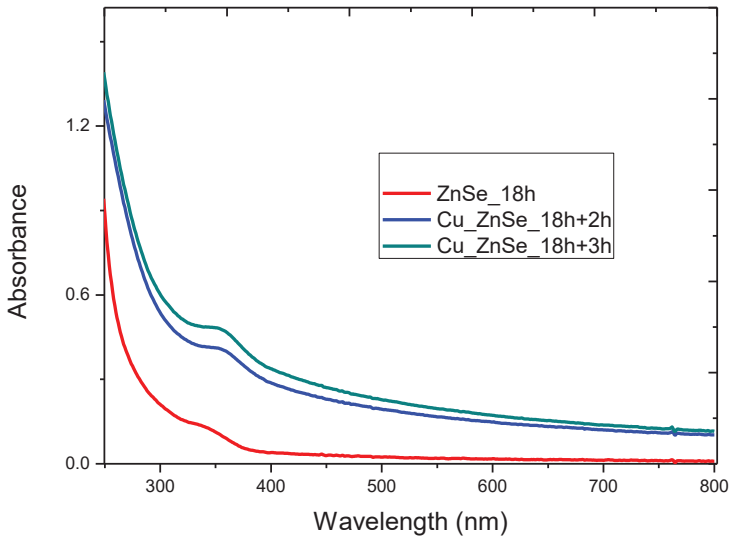

Figure 3.10 Absorption spectra of Cu doped ZnSe nanocrystals. The applied synthesis procedure was method a. Initial mol ratio of Zn:Cu was adjusted as 1:0.05.

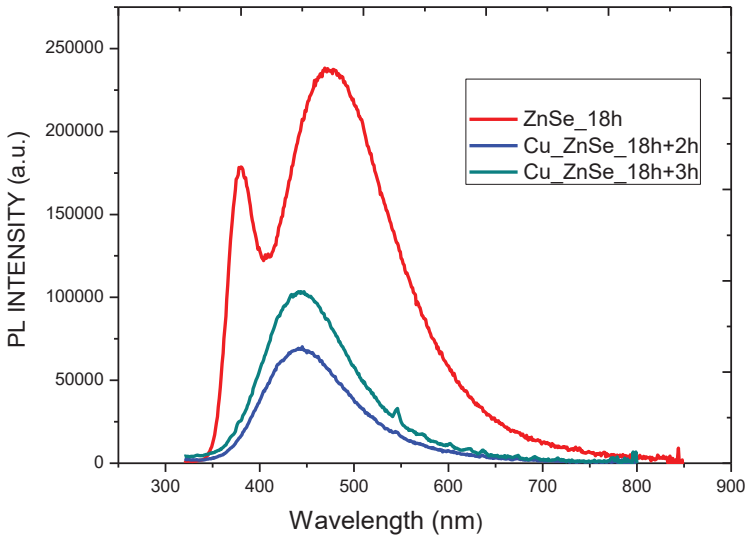

Figure 3.11 Photoluminescence spectra of Cu doped ZnSe NCs with respect to the reaction time.

After Cu doping, bandgap emission and defect emission peaks were disappeared while was occurred Cu related emission peak at 443 nm. And also position shifted from 473 nm to 443 nm. Gong et al, explained this situation briefly. In alkaline solution, the –SH groups can be partly decomposed to release sulfur to react with Zn^{2+} ions to form ZnS nanocrystals at the surface of QDs. This ZnS shell could be caused blue-shift in peak position.[29] Moreover, PL intensity increased in time, which can be also evidence that formed ZnS shell.

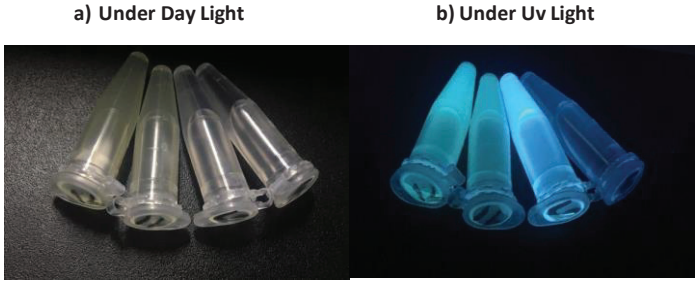

Figure 3.12 In figure a, from right to left image shows ZnSe (2h and 18h) respectively under the day light. In figure b, from right to left image shows Cu doped ZnSe (2h and 3h) nanocrystals under UV light.

As it shown Figure 3.12, after addition of Cu impurities, emission colors was blue-green color instead of green color like 2% Cu doped ZnSe NCs. It is also evidence that, forming ZnS shell while addition of Cu^{+2} ions.

Although the synthesis of doped nanocrystals is widely studied, there are impurities present on the nanocrystalline surface due to the mismatch between the NC crystal lattice and impurities. Therefore, these surface-doped NCs have poor luminescent stability because of impurities tend to separating from the nanocrystals surface. Moreover, internally doped Cu:ZnSe suffer from very weak chemical stability in the open air. there are several reasons for instability of Cu doped ZnSe such as environmental condition, Zn-MPA complexes in solution and pH variation.[24]

Wang et al, investigated the chemical stability of NCs in the different environmental conditions. They found that, after fifteen hours, Cu doped ZnSe nanocrystals formed white precipitate under the oxygen and photoirradiation. They suggest that, major composition of this precipitate can be $Zn(OH)_2$. After 40 hours, Cu doped ZnSe nanocrystals formed brown precipitates.(see in figure 3.13) The reason of this can be oxidation of Se^{-2}, and disulfide formation in the sample.

In figure 3.13 show that, the changed in the appearance of the Cu doped ZnSe nanocrystalline after two days. The reason could be this photophysical and photochemical processes during storage of NCs. Wong et al, explained this in various steps. When the photoelectric electron and holes are inactive by chemical reaction, the stability of the nanocrystals is poor.

Figure 3.13 show the 5% Cu doped ZnSe after two days. luminescence property of nanocrystals disappeared and also brown precipitate occured.

$$¼\ O_2 + ½\ H_2O + e \rightarrow OH^- \quad (3.1)$$

$$^-RS^- + h \rightarrow ½\ (RSSR^-) \quad (3.2)$$

Wong et al, explained the chemical reactions taking place as shown above. Under photoirradiation, photoinduced electrons consuming by oxygen via reaction 3.1. In the beginnig of reaction MPA ligands present in solution like Zn-MPA complexes. However, after during the storage, reaction 3.2 and 3.3 occured. $^-RS^-$ point out the MPA ligand capped on the ZnSe NC surface. The real form of MPA ligand exist on the NC surface is $ZnSR^-$. Produced disulfides are shown as $^-RSSR^-$. The disulfides produced as shown in reaction ii are replaced by free MPA ligands in solution. Because zinc's ability to bind disulfides is weaker than MPA.

$$½\ Se^{2-} + h \rightarrow ½\ Se \quad (3.3)$$

In the reaction 3.3 showed that, photoinduced holes declined while free MPA ligands will consumed. This situation results in nanocrystalline degradation.

The graphs have continued with the results of nanoparticles synthesized by the method of b. Due to the aggregation of 5% Cu doped ZnSe nanoparticles , the experiment was continued with 2% Cu doped ZnSe nanoparticles.

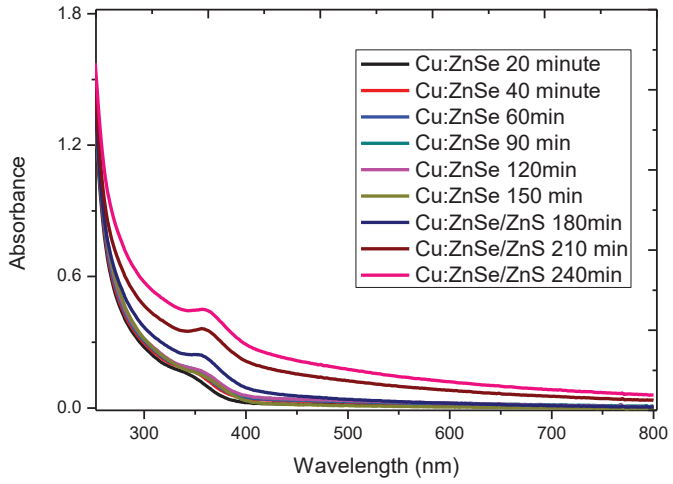

Figure 3.14 Absorption spectra of Cu doped ZnSe nanocrystals. The applied synthesis procedure was method b. Initial mol ratio of Zn:Cu was adjusted as 1:0.02.

Figure 3.14 show the absorption spectra of 2% Cu doped ZnSe nanocrystals. Absorbance spectra showed that, the addition of copper ions did not cause a very effective change in the absorbance band. However, covering of nanoparticles with ZnS shell provides to red shift from 355 nm to 362 nm. The reason of this could be the growth of nanocrystals after addition of the ZnS shell[32].

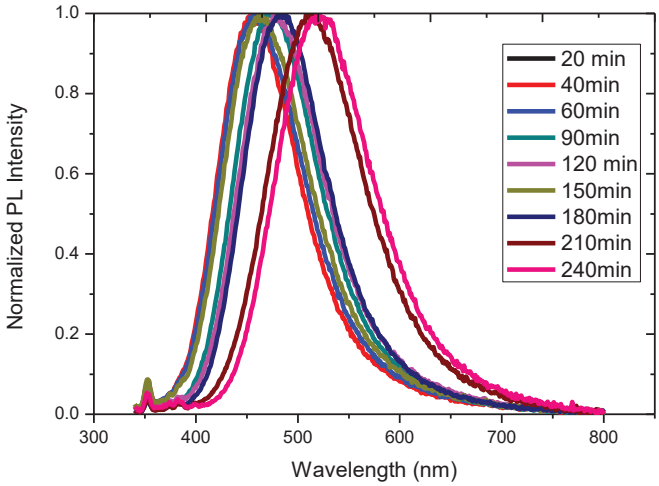

Figure 3.15 Normalized fluorescence spectrum of Cu doped ZnSe NCs with respect to the reaction time.

Figure 3.15 show the photoluminescence emission spectrum of 2% Cu doped ZnSe/ZnS nanocrystals were synthesized by using method b. The graph indicate that, there was no bandgap emission was observed for ZnSe:Cu NCs, whereas only the trap emission was exhibited. This result showed that the doping of a small quantity of Cu dopant increased the trap emission remarkably. The peak shifted from 455 nm to 520 nm with reaction time and the emission color change from blue to green. Cu dopant could be responsible for the redshift of the emission spectra, since the trap emission was less dependent on the NC size[32].

Photoluminescence Quantum Yield of Cu doped ZnSe nanocrystals were measured by using integrated sphere. Figure 3.16 show the photoluminescence quantum yield of ZnSe nanocrystals. PL QY % of ZnSe nanocrystals increased up to 20.8 % after 19 hour of reaction. Than decreased to 13 % during the reaction. This is also expectable that when the reaction time increases, size of nanocrystals also increase and some defect states started to form which causes the decrease in quantum yield of nanocrystals.

As shown in Figure 3.17, addition of copper ion to the ZnSe NCs caused to decreasing of the photoluminescence quantum yield of nanoparticles. The quantum yield of the Cu:ZnSe NCs began to decrease after 2 hours and the reduction continued throughout the reaction. The PL QY% of the Cu:ZnSe generally lower than ZnSe NCs because of the poor stability of Cu doped ZnSe nanocrystals[32]. However, after addition of shell the PL QY% of NCs increased up to 15.2 % (after 120 minute).

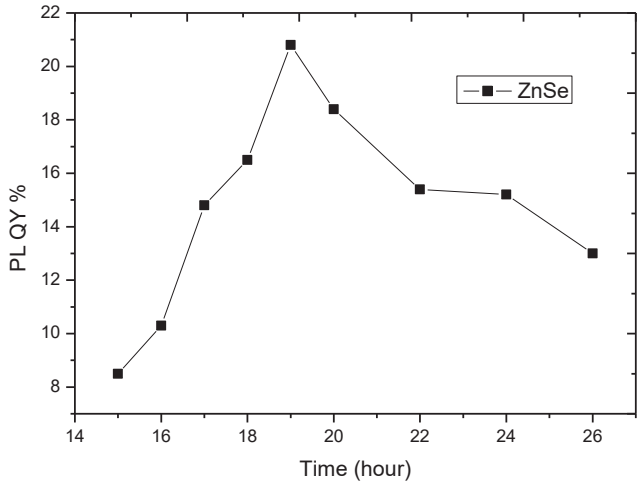

Figure 3.16 Photoluminescence Quantum Yield of ZnSe nanoparticles. After 19 hour of reaction, the PL QY % increased up to 20.8 %.

The instability of Cu doped ZnSe nanocrystals in oxygen and photoirridation were discussed under theFigure 3.13. In the presence of photoirridation, nanocrystals possess weak stability in an oxygen atmosphere. N_2 is an inert gas, which is unable to consume photoinduced electrons. Therefore, the nanocrystals synthesized by method b were stored by away from light and oxygen. However, even under nitrogen atmosphere and darkness, PL QY % of synthesized Cu doped ZnSe nanocrystals were decreased in a month. On the other hand, photoluminescence quantum yield of Cu doped ZnSe/ZnS nanocrystals were not changed in a month. Besides, Cu doped ZnSe/ZnS nanocrystals demonstrated good stability in a time.

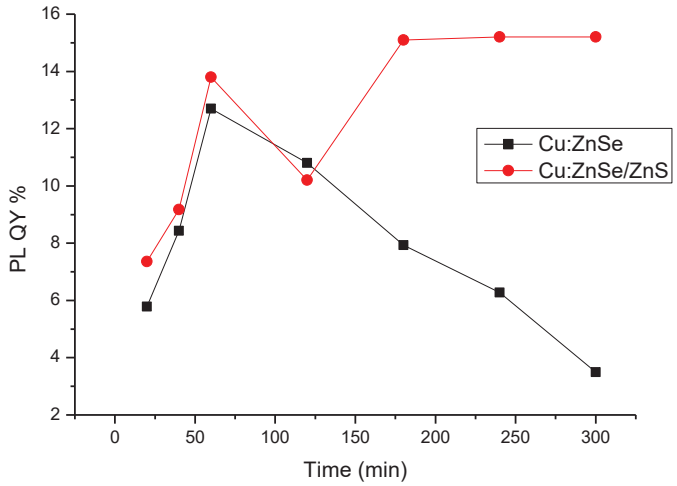

Figure 3.17 Photoluminescence Quantum Yield of Cu:ZnSe and Cu:ZnSe/ZnS nanoparticles. Addition of ZnS shell provided to improving quantum yield of nanoparticles.

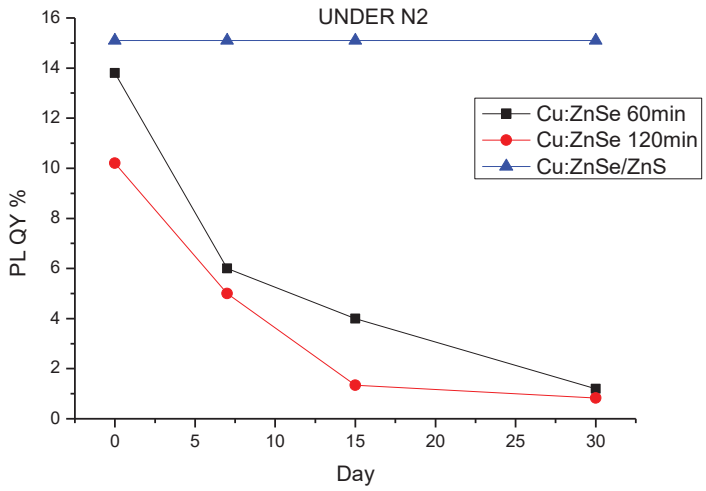

Figure 3.18 show the quantum yield of Cu:ZnSe NCs during the one moth under the N_2 atmosphere and in the dark.

3.3.2. Structural Characterization

Structural characterization was completed by Dynamic Light Scattering (DLS) instrument to obtain size of the nanocrystals, X-Ray diffraction (XRD) analysis to understand the structure of the nanocrystal and Scanning Electron Microscopy – Energy Dispersive X-Ray Spectroscopy (SEM-EDS) Instrument to get information about composition of the Cu and Mn doped ZnSe/ZnS nanocrystals.

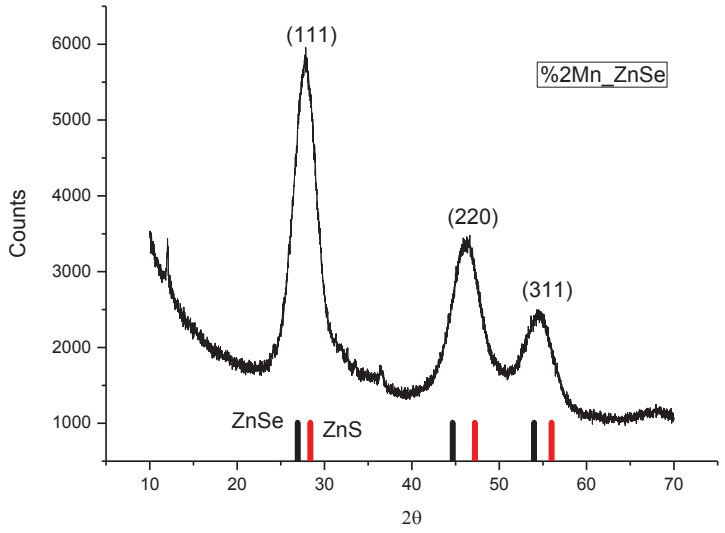

Figure 3.19 XRD patterns of synthesized %2 Mn doped ZnSe nanocrystals which are cubic and have zinc blende structure.

The XRD patterns of as-prepared Mn doped ZnSe QDs was shown in Figure 3.19. These diffraction features appearing at 27.8, 46.2, and 54.5 corresponded to the (111), (220), and (311) planes of cubic zinc blende structure. This results prove that, Mn doped ZnSe have a cubic zinc blend structure similar to undoped ZnSe QDs. Apparent shifts in 2-theta angles in the XRD patterns particularly for (220) and (311) planes were clearly seen. These findings indicate Mn^{2+} ions are mainly located on (220) and (311) planes. The reason why the Mn doped ZnSe crystal is present at a higher angle than the host ZnSe crystal is the formation of ZnS shell with smaller lattice due to the partial degradation of the MPA ligand.[28]

The elemental composition was obtained by SEM-EDS analysis. The SEM-EDS analysis were carried two weeks after the synthesis for Mn doped ZnSe/ZnS nanocrystals. SEM-EDS results are shown in Table 3.3.

Table 3.3 SEM-EDS results for Mn doped ZnSe and Mn doped ZnSe/ZnS nanocrystals two weeks after the synthesis.

Element	**Zn /Mn (Initial mole ratio)**	**Composition (from SEM-EDS)**
%2 Mn ZnSe	1:0.02	$Mn_{0.02}$ $Zn_{0.98}$ $Se_{0.55}$ $S_{0.45}$
%15 Mn ZnSe/ZnS	1:0.15	$Mn_{0.14}$ $Zn_{0.86}$ $Se_{0.57}$ $S_{0.43}$
%40 Mn ZnSe/ZnS	1:0.40	$Mn_{0.19}$ $Zn_{0.81}$ $Se_{0.35}$ $S_{0.65}$

SEM-EDS analysis confirmed that Mn^{2+} ions were doped into ZnSe nanocrystals. Zn, Se, S and Mn peaks originate from the doped core and core shell nanocrystals. However, 2% Mn doped ZnSe has S element because of capping MPA ligand.[28] By SEM-EDS measurements, the amount of Mn^{2+} ions with respect to Zn ion incorporated into the QDs as an atomic percent was calculated as 2, 14 and 19 % when the initial Mn^{2+} mole percentages were of 2, 15 and 40 %, respectively. This finding was interpreted as limited numbers of sites for Mn^{2+} ions for the incorporation into the lattice available.

Table 3.4 also confirmed the nature of materials. It is acceptable that the amount of Cu is greater than the amount added to the reaction. Because, according to the SEM-EDS interpretation, if the results (in weight %) are between 20-100 %, the error could be up to 5 %.

Dynamic Light Scattering is a common technique for determining particle size in colloidal suspensions. However, it can not able to measure exact size of the nanocrystal. DLS measures both the hard core and the hydrodynamic diameter of nanocrystals. Figure 3.16 showed size distribution of core ZnSe NCs, 2% Cu doped ZnSe and doped ZnSe/ZnS nanocrystals respectrively. Normally the hydrodynamic radius of ZnSe nanocrystalline is between 2.3 nm - 4.2nm.[28] In our case, core ZnSe NCs was measured as 10 nm. The reason of this could be agglomeration of particles in solution. After addition of copper dopant, the size of nanocrystals increasing 15 nm. After additon of shell, the nanocrystals were measured as 18 nm.

Table 3.4 EDS analysis of Cu doped ZnSe/ZnS nanocrystals after 2 weeks. Zn:Mn molar ratio was 1:0.02 respectively.

Element	**Zn /Mn (Initial mole ratio)**	**Composition (from SEM-EDS)**
%2 Cu ZnSe/ZnS	1: 0.02	$Cu_{0.02}\ Zn_{0.98}\ Se_{0.41}\ S_{0.59}$

In order to measure size of the Mn doped ZnSe/ZnS nanocrystals, both of the samples were centrifuged firstly. Then, samples were redispersed in water. Before the measurement, samples were sonicated and it was passed through microfilter. According to DLS result, 15% Mn doped ZnSe/ZnS nanocrystals was measured 15 nm and 40% Mn doped ZnSe/ZnS nanocrystals was measured 36 nm. The increase in the nanoparticle size is due to the formation of the ZnS shells and increasing initial Mn:Zn mole ratio both. This results also confirmed by SEM-EDS analysis.

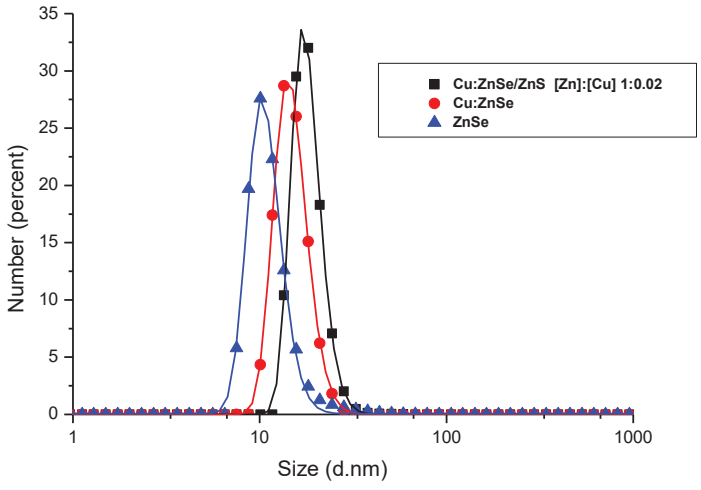

Figure 3.20 DLS result of ZnSe, Cu doped ZnSe and Cu:ZnSe/ZnS nanocrystals respectively.

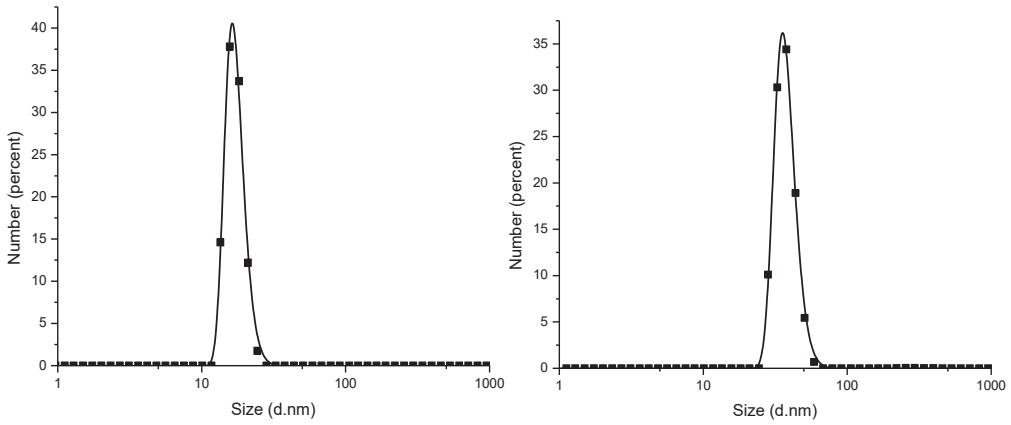

Figure 3.21 Size distribution of 15% and 40% Mn doped ZnSe/ZnS nanocrystals respectively. The hydrodynamic diameters of nanocrystals increased with the increase of Mn:Zn mole ratio.

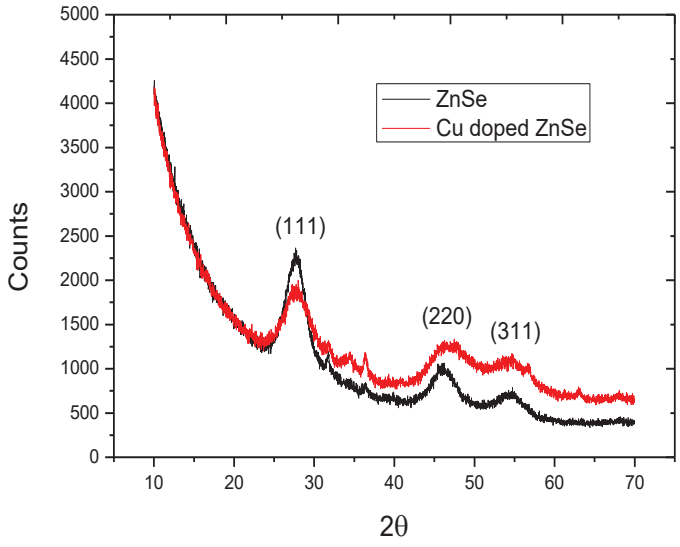

Figure 3.22 XRD patterns of synthesized 2 % Cu doped ZnSe nanocrystals which are cubic and have zinc blende structure.

The XRD pattern of Cu doped ZnSe and ZnSe NCs were showed in figure 3.18. The diffraction peaks of the QDs were found to be consistent with standard patterns of the cubic phases of ZnSe. Three main diffraction peaks of both samples appear approximately at 25.5, 46.1, and 54.3 corresponded to the (111), (220), and (311) planes

of cubic zinc blende structure. The broad diffraction peaks indicated the formation of nano-scaled particles[29].

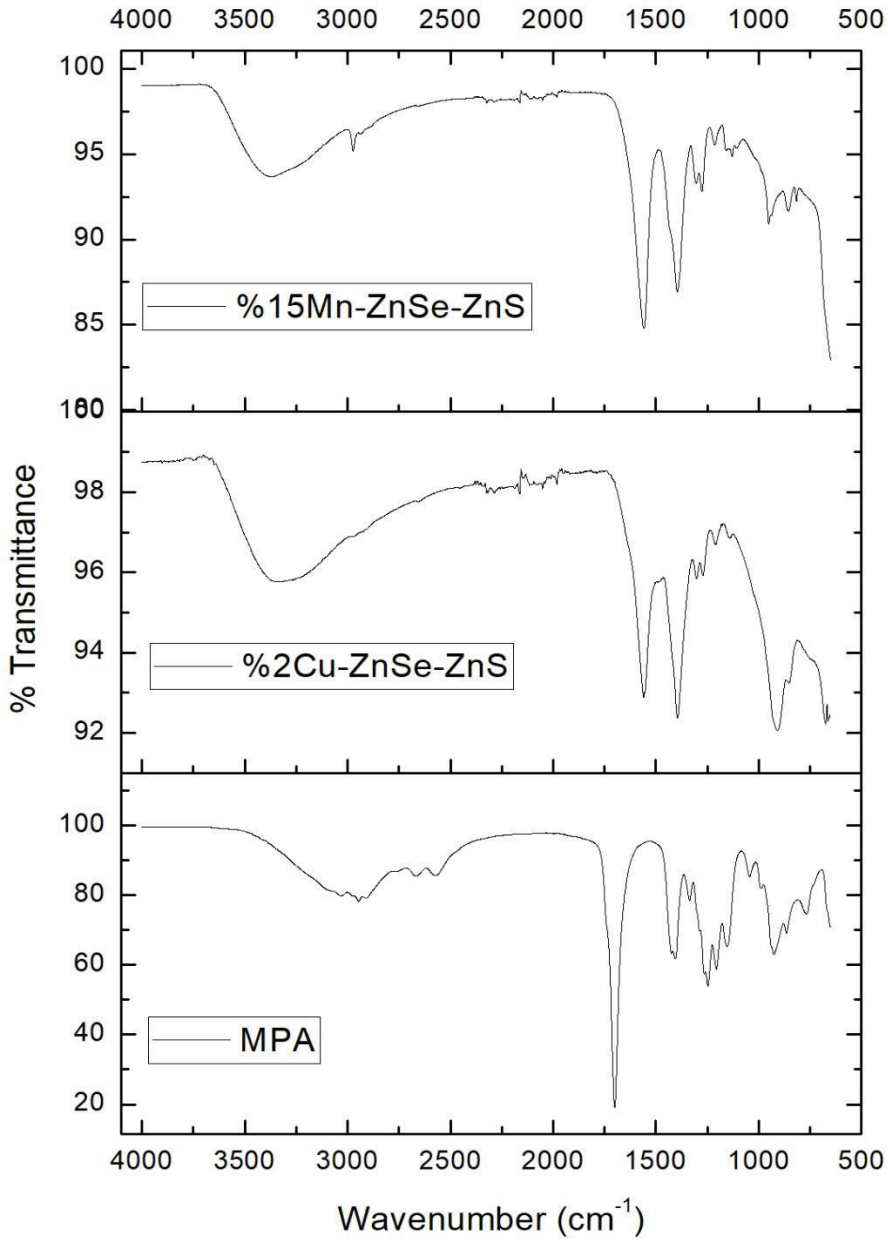

Figure 3.23 FTIR spectra of MPA, Cu doped ZnSe/ZnS NCs and Mn doped ZnSe/ZnS NCs respectively.

FT-IR spectra of the MPA ligand and of the purified and dried Mn doped ZnSe/ZnS and Cu doped ZnSe/ZnS NCs are given in Figure 3.23. The broad peak at 3150

cm^{-1} comes from O-H streching vibration and through the 1700 cm^{-1} C=O stretching vibration. [28] MPA ligand has S-H strech band between 2668 cm^{-1} and 2568 respectively. The disappearance of this band in the Cu and Mn doped ZnSe nanocrystalline indicates that the MPA ligand was bound to the surface by covalent bond. Besides, The MPA connected to the surface forms, symmetrical and asymmetric streching vibrations at 1400 cm^{-1} and 1567 cm^{-1} for Mn doped ZnSe/ZnS NCs respectively. Also the signal at 3380 cm-1 representing hydroxyl group of the acid function and the other bands at 2964 cm^{-1} representing the C-H stretching vibrations.

For Cu doped ZnSe/ZnS NCs, also show the MPA ligand was attached to the ZnSe surfaces. The bands appear at 1395 cm^{-1} and 1563 cm^{-1}. Between 2500 cm^{-1} and 3500^{-1} wavenumbers indicate the O-H group of the acid function.

CHAPTER 4
CONCLUSION

One pot aqueous synthesis method was used to synthesize MPA capped Cu and Mn doped ZnSe/ZnS nanocrystals. We investigated the effect of different dopant ions to the ZnSe nanocrystals. As-prepared 2%, 5% and 40% Mn doped ZnSe show that, inceasing initial Zn:Mn mole ratio caused to decrease PL intensity. The introduction of ZnS shell at the surface of the Mn doped ZnSe QDs improved their photoluminescence properties, resulting in stronger emission. The molar ratio of Zn:Mn 1:0.15 gives the best result in terms of photoluminesce decay traces and quantum yield measurements. XRD was performed to obtain structural information about nanocrystals that Mn doped ZnSe/ZnS nanocrystals are cubic have zinc blende structure. Compositional information obtained from SEM-EDS.

The emission spectra showed that the band emission of ZnSe QDs almost disappeared after doping of 2 % $Cu^{2+,}$ instead, appeared the fluorescence emission peak of $Cu^{2+.}$ However, if the dopant concentration was increased, PL intensity was quenched and luminescence property of NCs was disappeared. The XRD result showed that Cu doped ZnSe nanocrystals are cubic zinc blende structure.

Since Cu doped ZnSe is very sensitive to air, luminescence property has decreased in hours. The reason of this situation, is storage of NCs in oxygen under photoirradiation was discussed in detail. Therefore, the Cu doped ZnSe nanocrystals synthesized by method b, were storage under the nitrogen atmosphere and in the dark. However, quantum yields of one-hour and two-hour samples decreased over time whereas Cu doped ZnSe/ZnS nanocrystals exhibited good stability and unchanged quantum yields in the time.

REFERENCES

1. Hughes, M. P. J. N., AC electrokinetics: applications for nanotechnology. **2000,** *11* (2), 124.

2. Society, R.; Engineering, R. A. o., *Nanoscience and Nanotechnologies: Opportunities and Uncertainties*. Royal Society: 2004.

3. Jing, L.; Kershaw, S. V.; Li, Y.; Huang, X.; Li, Y.; Rogach, A. L.; Gao, M. J. C. r., Aqueous based semiconductor nanocrystals. **2016,** *116* (18), 10623-10730.

4. Mansur, H. S., Quantum dots and nanocomposites. **2010,** *2* (2), 113-129.

5. Murray, C.; Norris, D. J.; Bawendi, M. G. J. J. o. t. A. C. S., Synthesis and characterization of nearly monodisperse CdE (E= sulfur, selenium, tellurium) semiconductor nanocrystallites. **1993,** *115* (19), 8706-8715.

6. Mirzaei, J.; Reznikov, M.; Hegmann, T. J. J. o. M. C., Quantum dots as liquid crystal dopants. **2012,** *22* (42), 22350-22365.

7. Hines, M. A.; Guyot-Sionnest, P., Synthesis and Characterization of Strongly Luminescing ZnS-Capped CdSe Nanocrystals. *The Journal of Physical Chemistry* **1996,** *100* (2), 468-471.

8. Zhang, F.; He, X.-W.; Li, W.-Y.; Zhang, Y.-K. J. J. o. M. C., One-pot aqueous synthesis of composition-tunable near-infrared emitting Cu-doped CdS quantum dots as fluorescence imaging probes in living cells. **2012,** *22* (41), 22250-22257.

9. Samokhvalov, P.; Artemyev, M.; Nabiev, I. J. C. A. E. J., Basic principles and current trends in colloidal synthesis of highly luminescent semiconductor nanocrystals. **2013,** *19* (5), 1534-1546.

10. Regulacio, M. D.; Han, M.-Y. J. A. o. c. r., Composition-tunable alloyed semiconductor nanocrystals. **2010,** *43* (5), 621-630.

11. Zhong, X.; Han, M.; Dong, Z.; White, T. J.; Knoll, W., Composition-Tunable ZnxCd1-xSe Nanocrystals with High Luminescence and Stability. *Journal of the American Chemical Society* **2003,** *125* (28), 8589-8594.

12. Sharma, S. N.; Sharma, H.; Singh, S.; Mehra, R. M.; Singh, G.; Shivaprasad, S. M., Single pot synthesis of composition tunable CdSe–ZnSe (core–shell) and ZnxCd1–xSe (ternary alloy) nanocrystals with high luminescence and stability. *Materials Research Innovations* **2010,** *14* (1), 62-67.

13. Wang, M.; Tang, A.; Zhu, D.; Yang, C.; Teng, F., Understanding the roles of metal sources and dodecanethiols in the formation of metal sulfide nanocrystals via a two-phase approach. *CrystEngComm* **2015,** *17* (34), 6598-6606.

14. Pan, D.; Jiang, S.; An, L.; Jiang, B. J. A. M., Controllable Synthesis of Highly Luminescent and Monodisperse CdS Nanocrystals by a Two-Phase Approach under Mild Conditions. **2004,** *16* (12), 982-985.

15. Pan, D.; Wang, Q.; Jiang, S.; Ji, X.; An, L. J. A. M., Synthesis of Extremely Small CdSe and Highly Luminescent CdSe/CdS Core–Shell Nanocrystals via a Novel Two-Phase Thermal Approach. **2005,** *17* (2), 176-179.

16. Rogach, A. L.; Franzl, T.; Klar, T. A.; Feldmann, J.; Gaponik, N.; Lesnyak, V.; Shavel, A.; Eychmüller, A.; Rakovich, Y. P.; Donegan, J. F., Aqueous Synthesis of Thiol-Capped CdTe Nanocrystals: State-of-the-Art. *The Journal of Physical Chemistry C* **2007,** *111* (40), 14628-14637.

17. Fu, S. S.; Sun, Q. Z.; Li, D. Y.; Dong, M. T.; Liu, S. X.; Huang, C. B., A Novel One-Pot Synthesis of UV-Blue ZnSe Nanocrystals in Aqueous Solution. *J. Chin. Chem. Soc.* **2013,** *60* (3), 309-313.

18. Fery-Forgues, S.; Lavabre, D., Are Fluorescence Quantum Yields So Tricky to Measure? A Demonstration Using Familiar Stationery Products. *Journal of Chemical Education* **1999,** *76* (9), 1260.

19. Qian, H.; Dong, C.; Peng, J.; Qiu, X.; Xu, Y.; Ren, J., High-quality and water-soluble near-infrared photolumineseent CdHgTe/CdS quantum dots prepared by adjusting size and composition. *J. Phys. Chem. C* **2007,** *111* (45), 16852-16857.

20. Xue, G.; Chao, W.; Lu, N.; Xingguang, S., Aqueous synthesis of Cu-doped ZnSe quantum dots. *Journal of Luminescence* **2011,** *131* (7), 1300-1304.

21. Senthilkumar, K.; Kalaivani, T.; Kanagesan, S.; Balasubramanian, V., Synthesis and characterization studies of ZnSe quantum dots. *J. Mater. Sci.-Mater. Electron.* **2012,** *23* (11), 2048-2052.

22. Zhang, S. L.; Lin, C. F.; Weng, Y. L.; He, L. C.; Guo, T. L.; Zhang, Y. A.; Zhou, X. T., Facile and green synthesis of core-shell ZnSe/ZnS quantum dots in aqueous solution. *J. Mater. Sci.-Mater. Electron.* **2018,** *29* (19), 16805-16814.

23. Zhang, W. J.; Li, Y.; Zhang, H.; Zhou, X. G.; Zhong, X. H., Facile Synthesis of Highly Luminescent Mn-Doped ZnS Nanocrystals. *Inorganic Chemistry* **2011,** *50* (20), 10432-10438.

24. Wang, C.; Xu, S.; Wang, Z.; Cui, Y., Key Roles of Impurities in the Stability of Internally Doped Cu:ZnSe Nanocrystals in Aqueous Solution. *The Journal of Physical Chemistry C* **2011,** *115* (38), 18486-18493.

25. Zhang, Y. P.; Shen, Y. H.; Wang, X. F.; Zhu, L.; Han, B.; Ge, L. L.; Tao, Y. L.; Xie, A. J., Enhancement of blue fluorescence on the ZnSe quantum dots doped with transition metal ions. *Mater. Lett.* **2012,** *78*, 35-38.

26. Shuhong, X.; Chunlei, W.; Zhuyuan, W.; Haisheng, Z.; Jing, Y.; Qinying, X.; Haibao, S.; Rongqing, L.; Wei, L.; Yiping, C., Aqueous synthesis of internally doped Cu:ZnSe/ZnS core–shell nanocrystals with good stability. *Nanotechnology* **2011,** *22* (27), 275605.

27. Luong, B. T.; Hyeong, E.; Yoon, S.; Choi, J.; Kim, N., Facile synthesis of UV-white light emission ZnSe/ZnS:Mn core/(doped) shell nanocrystals in aqueous phase. *RSC Advances* **2013,** *3* (45), 23395-23401.

28. Aboulaich, A.; Geszke, M.; Balan, L.; Ghanbaja, J.; Medjahdi, G.; Schneider, R., Water-Based Route to Colloidal Mn-Doped ZnSe and Core/Shell ZnSe/ZnS Quantum Dots. *Inorganic Chemistry* **2010,** *49* (23), 10940-10948.

29. Gong, F. Z.; Sung, L.; Ruan, H.; Cai, H. M., Hydrothermal synthesis and photoluminescence properties of Cu-doped ZnSe quantum dots using glutathione as stabilizer. *Mater. Express* **2018,** *8* (2), 173-181.

30. Zheng, Y.; Yang, Z.; Ying, J. Y., Aqueous Synthesis of Glutathione-Capped ZnSe and Zn1–xCdxSe Alloyed Quantum Dots. **2007,** *19* (11), 1475-1479.

31. Dong, B.; Cao, L.; Su, G.; Liu, W., Facile synthesis of highly luminescent UV-blue emitting ZnSe/ZnS core/shell quantum dots by a two-step method. *Chemical Communications* **2010,** *46* (39), 7331-7333.

32. Han, J. S.; Zhang, H.; Tang, Y.; Liu, Y.; Yao, X.; Yang, B., Role of Redox Reaction and Electrostatics in Transition-Metal Impurity-Promoted Photoluminescence Evolution of Water-Soluble ZnSe Nanocrystals. *J. Phys. Chem. C* **2009,** *113* (18), 7503-7510.